

Stockholm, 31-10-2019

Re.: Revised version of manuscript BG-2019-89

Dear Associate Editor,

I have uploaded the revised version of the manuscript as a word file of the main text, with all changes highlighted in track changes (including tables and figures), as well as a pdf of the revised supplement.

I believe we have addressed all concerns made in the reviews and the one interactive comment that we suggested in our Author's response.

There were some technical/formatting changes requested by the reviewers, most significantly:

- 1) To remove Figure 2, because these regressions were also included in Figure 3, etc
- 2) To prepare a Table S2 for Supplementary Materials that summarizes landscape representation in each experiment/study area
- 3) To move paragraphs in results to methods, particularly the ones explaining the division of the datasets into landscape classes (and their subdivisions in the PAGE21 experiment)
- 4) To add number of samples (and, in some cases, legends) in the Figures

As for the text, following the main concerns raised in the reviews, the most important changes are:

- 5) Expanded method description for the CryoCarb experiment
- 6) Expanded discussion

Detailed summary of most important changes:

Line 3:	Added co-author
L54-58	Added statements
L182-183	Added statement
L195-234	Additional details for CryoCarb experiment
L285-287	Added Table S2
L288-299	From results to methods
L317-327	From results to methods
L352 + L362	Added number of samples for each regression
L385	Removed Figure 2
L540	Small error in slope value for PAGE21 Pt, corrected 0.20 to 0.24, 0.14 to 0.17
L691-698 + L708-749	Added discussion paragraphs
L840+	Added references
Figures 2, S3-S5	Added number of samples
Figures 3 and 4	Added legends and number of samples, Change in symbol and color regression line in Fig. 3d

We hope you find these revisions adequate.

Kind regards, Peter Kuhry

1 Lability classification of soil organic matter in the northern permafrost region

2
3 *Kuhry, P.¹, Bárta, J.², Blok, D.³, Elberling, B.⁴, Faucherre, S.⁴, Hugelius, G.^{1,5}, Jørgensen, C. J.^{4,6},
4 Richter, A.^{6,7}, Šantrůčková, H.² and Weiss, N.^{1,7,8}*

5
6 ¹⁾ *Department of Physical Geography, Stockholm University, Sweden*

7 ²⁾ *Department of Ecosystem Biology, University of South Bohemia, Ceske Budejovice, Czech Republic*

8 ³⁾ *Department of Physical Geography and Ecosystem Science, Lund University, Sweden*

9 ⁴⁾ *Center for Permafrost (CENPERM), Department of Geosciences and Natural Resource Management, University of*
10 *Copenhagen, Denmark*

11 ⁵⁾ *Bolin Centre for Climate Research, Stockholm University, Sweden*

12 ⁶⁾ *Current affiliation: Department of Bioscience, Section for Arctic Environment, Aarhus University, Denmark*

13 ⁷⁾ *Department of Microbiology and Ecosystem Science, University of Vienna, Austria*

14 ^{7,8)} *Current affiliation: Department of Geography and Environmental Studies, Wilfrid Laurier University, Yellowknife,*
15 *Canada*

16
17 Correspondence email: peter.kuhry@natgeo.su.se

18 19 Abstract

20
21 The large stocks of soil organic carbon (SOC) in soils and deposits of the northern permafrost region
22 are sensitive to global warming and permafrost thawing. The potential release of this carbon (C) as
23 greenhouse gases to the atmosphere does not only depend on the total quantity of soil organic matter
24 (SOM) affected by warming and thawing, but also on its lability (i.e. the rate at which it will decay).
25 In this study we develop a simple and robust classification scheme of SOM lability for the main
26 types of soils and deposits ~~of~~ in the northern permafrost region. The classification is based on widely
27 available soil geochemical parameters and landscape unit classes, which makes it useful for
28 upscaling to the entire northern permafrost region. We have analyzed the relationship between C
29 content and C-CO₂ production rates of soil samples in two different types of laboratory incubation
30 experiment. In one experiment, c. 240 soil samples from four study areas were incubated using the
31 same protocol (at 5 °C, aerobically) over a period of one year. Here we present C release rates
32 measured on day 343 of incubation. These long-term results are compared to those obtained from
33 short-term incubations of c. 1000 samples (at 12 °C, aerobically) from an additional three study
34 areas. In these experiments, C-CO₂ production rates were measured over the first four days of
35 incubation. We have focused our analyses on the relationship between C-CO₂ production per gram
36 dry weight per day (μgC-CO₂ gdw⁻¹ d⁻¹) and C content (%C of dry weight) in the samples, but show
37 that relationships are consistent when using C/N ratios or different production units such as μgC per
38 gram soil C per day (μgC-CO₂ gC⁻¹ d⁻¹) or per cm³ of soil per day (μgC-CO₂ cm⁻³ d⁻¹). C content of
39 the samples is positively correlated to C-CO₂ production rates but explains less than 50 % of the
40 observed variability when the full datasets are considered. A partitioning of the data into landscape
41 units greatly reduces variance and provides consistent results between incubation experiments. These
42 results indicate that relative SOM lability decreases in the order: Late Holocene eolian deposits >
43 alluvial deposits and mineral ~~upland~~ soils (including peaty wetlands) > Pleistocene Yedoma deposits
44 > C-enriched pockets in cryoturbated soils > peat deposits. Thus, three of the most important SOC
45 storage classes in the northern permafrost region (Yedoma, cryoturbated soils and peatlands) show
46 low relative SOM lability. Previous research has suggested that SOM in these pools is relatively
47 undecomposed and the reasons for the observed ~~resistance to~~ low rates of decomposition in our

48 experiments need urgent attention if we want to better constrain the magnitude of the thawing
49 permafrost carbon feedback on global warming.

51 1. Introduction

53 Permafrost has been recognized as one of the vulnerable carbon (C) pools in the Earth System
54 (Gruber et al., 2004). A recent report of the International Panel on Climate Change (IPCC, 2018)
55 identifies the thawing permafrost carbon-climate feedback as one of the key uncertainties when
56 assessing global emission targets to keep global warming under 1.5 (2) °C. Furthermore, the urgency
57 of additional research is highlighted by the fact that most permafrost in the northern circumpolar
58 region has already experienced warming in recent decades (Biskaborn et al., 2019).

59 In the ~~most recent~~last decade there has been a surge in papers dealing with the permafrost
60 carbon feedback on climate change (e.g. Schuur et al., 2008; Kuhry et al., 2010). This increased
61 interest was fueled by a new and high estimate of the total soil organic carbon (SOC) storage in the
62 northern permafrost region (Tarnocai et al., 2009), which was received with great interest by the
63 Earth System Science community (e.g., Ciais, 2009). Since this first new estimate was published, a
64 multitude of new SOC inventories at the landscape level have been conducted across the
65 Circumpolar North (e.g. Hugelius and Kuhry, 2009; Hugelius et al., 2010; Horwath Burnham and
66 Sletten, 2010; Palmtag et al., 2015; Gentsch et al., 2015a; Siewert et al., 2016). Recent studies have
67 also focused on re-evaluating the spatial extent and SOC storage of the Yedoma 'Ice Complex' and
68 Alas deposits (Strauss et al., 2013; Walter-Anthony et al., 2014; Hugelius et al., 2016; Shmelev et al.,
69 2017).

70 This new data has prompted an update of the total SOC storage in the northern permafrost
71 region, its vertical partitioning and its broad (continental scale) distribution (Hugelius et al., 2014).
72 The new estimate amounts to c. 1400 PgC for the top 3 m of soils and deeper deposits, including
73 permafrost and non-permafrost organic soils (Histels/Histosols, 302 PgC), cryoturbated permafrost
74 mineral soils (Turbels, 476 PgC), non-cryoturbated permafrost mineral soils (Orthels) and non-
75 permafrost mineral soils (256 PgC), and deeper Yedoma (301 PgC, >300 cm) and Delta (91 PgC,
76 >300 cm) deposits. The spatial distribution of SOC stocks according to the major permafrost soil
77 (Gelisol) suborders, non-permafrost mineral soils and Histosols (Soil Survey Staff, 2010) is
78 graphically represented in the updated version of the Northern Circumpolar Soil Carbon Database
79 (NCSCDv2, 2014).

80 The importance of an accurate estimate of total SOC storage in the northern permafrost region is
81 illustrated by a recent review of the permafrost carbon feedback (Schuur et al., 2015), which
82 included a comparison of future C release in a total of eight Earth System models (~~ESMs~~). The
83 magnitude of the projected cumulative C loss from ~~thawing the~~ permafrost region by 2100, largely
84 based on the RCP 8.5 scenario (IPCC, 2013), varied greatly between models from 37 to 174 PgC.
85 However, by normalizing for the initial ~~permafrost~~C pool size in the different ~~models~~ESMs, the
86 proportional C loss from the permafrost zone was constrained to a much narrower range of $15 \pm 3 \%$
87 of the initial pool. This indicates that the quantity of SOC is a primary control when assessing C
88 losses from the northern permafrost region.

89 The magnitude of the permafrost carbon feedback, however, will not only depend on the rate of
90 future global warming (and its polar amplification), its effect on gradual and abrupt permafrost
91 thawing (Grosse et al., 2011), or the total size (and vertical distribution) of the permafrost SOC pool.
92 As shown by Burke et al. (2012), based on simulations with the Hadley Centre climate model,
93 quality (decomposability) parameters need also to be considered. Thus, in terms of C pool
94 parameters, the potential C release from the northern permafrost region will depend not only on SOC
95 quantity but also on soil organic matter lability (i.e. the rate at which SOM will decay following

96 warming and thawing). An important tool to assess potential C release from permafrost soils and
97 deposits are laboratory incubation experiments that consider both different types of substrate (e.g.,
98 Schädel et al., ~~2013~~2014) and time of incubation (e.g. Elberling et al., 2013).

99 The aim of this study is to add a measure of SOM lability to the current estimates of SOC
100 quantity, in order to define vulnerable C pools across the northern circumpolar region. We focus on
101 the relationship between solid phase geochemical parameters (particularly C content) and C release
102 rates in laboratory incubations of active layer and thawed permafrost samples from the main types of
103 soils and deposits found in the northern permafrost region. Our objective is to develop a SOM
104 lability classification scheme based on widely reported soil geochemical parameters in field SOC
105 inventories and general landscape classes, that can be linked to existing spatial SOC databases such
106 as the NCSCD (Tarnocai et al., 2009; Harden et al., 2012; Hugelius et al., 2014). We test the
107 robustness of our SOM lability classification by comparing two very different types of incubation
108 experiment, both in setup as well as timing of C release measurements.

110 2. Materials and methods

112 *2.1. Study areas*

114 The samples used in the incubation experiments were collected as part of landscape-level inventories
115 carried out in the context of the EU PAGE21 and ESF CryoCarb projects to assess total storage,
116 landscape partitioning and vertical distribution of SOC stocks in study areas across the northern
117 permafrost region. SOC storage data from these areas are presented in Weiss et al. (2017) for
118 Svalbard, Siewert et al. (2016) for Lena Delta, Palmtag et al. (2016) for Taymyr Peninsula, Palmtag
119 et al. (2015) for Lower Kolyma, Hugelius et al. (2011) for Seida, and Siewert (2018) for Stordalen
120 Mire. The location of all study areas is shown in Figure 1. The Lower Kolyma experiment includes
121 samples from two nearby located study areas (Shalaurovo and Cherskiy); the Taymyr Peninsula
122 experiment also includes samples from two nearby located study areas (Ary-Mas and Logata).
123 Metadata for each of these areas, including geographic coordinates, permafrost and vegetation zones,
124 climate parameters, number of soil profiles and incubated samples, type of incubation experiment,
125 and time of field collection, are presented in Table S1 (Supplementary Materials).

127 Figure 1. Location of study areas in northern Eurasia. PAGE21 experiment (Ny Ålesund,
128 Adventdalen, Stordalen Mire, Lena Delta); CryoCarb 1-Kolyma experiment (Shalaurovo,
129 Cherskiy); CryoCarb 2-Taymyr experiment (Ary-Mas, Logata); CryoCarb 3-Seida experiment.
130 Permafrost zones according to Brown et al. (1997).

132 *2.2. Field methods*

134 The sampling strategy applied for SOC field inventories was aimed at capturing all major landscape
135 units in each of the study areas, while at the same time ensuring an unbiased selection of soil profile
136 location. This semi-random sampling approach consisted of deciding on the positioning of generally
137 1 or 2 km long transects that crossed all major landscape units, with a strictly equidistant sampling
138 interval at normally 100 or 200 m that eliminated any subjective criteria for the exact location of
139 each soil profile. For SOC storage calculations, the mean storage in each landscape unit class was
140 weighed by its proportional representation in the study area based on remote sensing land cover
141 classifications.

142 At each soil profile site, the topsoil organic layer was collected by cutting out blocks of known
143 volume in three random replicates to account for spatial variability. These samples do not always
144 strictly adhere to the definition of an 'O' soil genetic horizon, because in areas with thin topsoil
145 organics (like in floodplains and mountain terrain) there can be a large admixture of minerogenic
146 material resulting in C contents of less than 12 %. Active layer samples were collected from
147 excavated pits by horizontally inserting fixed-volume cylinders. The permafrost layer was sampled
148 by hammering a steel pipe of known diameter incrementally into the ground, retrieving intact
149 samples for each depth interval. Depths intervals are normally 5 to 10 cm or less (e.g., when the
150 topsoil organic layer was very thin). The standard sampling depth was to 1 m below the soil surface;
151 at some sites it was not possible to reach this depth due to large stones in the soil matrix or thin soil
152 overlying bedrock (often in mountainous settings).

153

154 2.3. Incubation experiments

155

156 2.3.1. The PAGE21 incubation experiment

157

158 The PAGE21 incubation experiment was carried out at the University of Copenhagen (Denmark).
159 This experiment included one sample from the topsoil organics, one sample from the middle of the
160 active layer and one sample from the upper permafrost layer (normally 10-15 cm below the upper
161 permafrost table) from all mineral soil profiles collected in three of the PAGE21 study areas ([Ny](#)
162 [Ålesund](#), [Adventdalen](#) and [Lena Delta](#)). Samples were selected based on depth criteria and not any
163 specific soil characteristic (e.g., presence of C-enriched cryoturbated material or absence of excess
164 ground ice). In some cases, upper permafrost samples could not be collected due to very deep active
165 layers and/or thin soils (particularly in mountain settings). Peat samples are available from a fourth
166 PAGE21 study area ([Stordalen Mire](#)). In total c. 240 soil samples from four study areas across the
167 northern permafrost region (Ny Ålesund and Adventdalen, Svalbard; Stordalen Mire, N Sweden;
168 Lena Delta, N Siberia) were incubated in one and the same experiment (Faucherre et al., 2018).

169 The Dry Bulk Density (DBD) of samples used for incubation was measured at Stockholm
170 University (Sweden). The %C and %N of dry weight of the incubated samples were measured in an
171 elemental analyzer (EA Flash 2000, Thermo Scientific, Bremen, Germany) at the University of
172 Copenhagen (Denmark).

173 Samples were kept in frozen condition from collection until the start of the laboratory incubation
174 experiment. Samples were incubated at 5 °C and field water content levels (aerobic conditions) over
175 a one-year time period. Mean volumetric water content varied between 30 % (topsoil organics), 45-
176 50 % (active layer and permafrost layer mineral soil) and 69 % (peat). [In the original PAGE21](#)
177 [experiment \(Faucherre et al., 2018\)](#), C-CO₂ production rates were measured at five different
178 occasions between 7 to 343 days after the start of the experiment, using a nondispersive infrared LI-
179 840A CO₂/H₂O Gas analyzer (LICOR® Biosciences). Since all samples from all study areas were
180 processed and incubated using the same protocol, results are directly comparable. [Here](#)[In this study](#),
181 we use [the C release rates after nearly one year on day 343 of incubation as a measure of SOM](#)
182 [lability. These results, therefore, mostly address the 'slow' \(Schädel et al., 2014\) and 'stable'](#)
183 [\(Knoblauch et al., 2013\) SOM pools, with C cycling typically within a timespan of a \(few\) decade\(s\).](#)

184

185 2.3.2. The CryoCarb incubation experiments

186

187 The CryoCarb incubations were carried out at the University of South Bohemia (Ceske Budovice,
188 Czech Republic). These experiments included all samples from all profiles collected in each of three

189 study areas (CryoCarb 1-Kolyma in NE Siberia; CryoCarb 2-Taymyr in N Siberia; and CryoCarb 3-
190 Seida in NE European Russia). In total c. 1000 samples were incubated.

191 The Dry Bulk Density (DBD) of samples used for incubation was measured at Stockholm
192 University (Sweden). The %C and %N of dry weight were measured in an EA 1110 Elemental
193 Analyzer (CE Instruments, Milan, Italy) at Stockholm University (Seida samples) and the University
194 of Vienna (Kolyma and Taymyr samples).

195 The CryoCarb 1-Kolyma and CryoCarb-2 Taymyr samples were stored in a ground pit dug into
196 the active layer for up to two weeks, before further processing. Active layer samples would be little
197 impacted by this storage under ‘natural’ conditions, but (some of) the gradually thawing permafrost
198 layer samples might have experienced initial decay. CryoCarb 3-Seida samples collected in 2009
199 were kept in frozen storage for c. 10 years (see Table S1), before further processing.

200 In the laboratory, Collected soil samples were dried at 40-50 °C within two weeks after field
201 sampling (or retrieval from cold storage) and kept in a cold room (at 4 °C) until analyzed. For each
202 sample, 0.2g of dry soil was inoculated with 0.003-0.008g of soil inoculum in 1.6 ml of water
203 (soil:H₂O, 1:100, weight/volume) in 10 ml vacutainers, after which the vacutainers were
204 hermetically closed and the soil slurry was incubated in an orbital shaker at 12 °C for 96 hours. At
205 the end of incubation, CO₂ concentration in the headspace was analyzed using an HP 5890 gas
206 chromatograph (Hewlett-Packard, USA), equipped with a TC detector.

207 The study area and layer specific composite soil inoculi were prepared from fresh soil taken
208 separately from topsoil organic layer, mineral active layer, peat active layer, mineral permafrost layer
209 and peat permafrost layer, from multiple soil profiles collected in each study area. The Ffresh soil
210 was kept in a cold room (at 4 °C) and then conditioned at 15 °C for one week before inoculum
211 preparation. We consider that the small dry weight of our soil inoculi (which, in turn, have <2%
212 microbial biomass) has no significant impact on our C release measurements. The viability of inoculi
213 was checked by incubation in water and measuring its respiration.

214 The short term C-CO₂ production rates measured in the CryoCarb experiments most likely
215 address the ‘fast’ (Schädel et al., 2014) and ‘labile’ (Knoblauch et al., 2013) SOM pools, which
216 represent a small fraction of the total pool and decompose within a (few) year(s)., short term C-CO₂
217 production rates after rewetting of dried soil samples was used as an indicator of SOM lability. The
218 CryoCarb approach is based on the so-called ‘Birch effect’ (Birch, 1958), showing that after a
219 dry/wet cycle CO₂ mineralization increases. The extra C originates from mineralization of available
220 C released from organo-mineral complexes and dead biomass. In our sample pretreatment with rapid
221 drying at ≤ 50 °C we expect that a larger part of biomass died and decomposed already during this
222 process, which should therefore not severely affect our later measurements. Fierer and Schimel
223 (2003) showed that a substantial part of the released C can also come from microbial biomass which
224 died due to the osmotic shock after rewetting of soil. However, in their case, samples were dried at
225 room temperature resulting in less of a shock in the drying process to the microbial community. Our
226 measurements could have been affected by limitation of C mineralization due to the small size of
227 surviving biomass, which we overcame by inoculation with living cells. The principle of the ‘Birch
228 Effect’ is still used in ecological studies ranging from large scale carbon cycling in ecosystems to
229 detailed studies of SOC availability (e.g. Jarvis et al., 2007). It is well documented that the amount of
230 extra C released after rewetting of dry soil is site and soil type specific and represents an easily
231 available fraction of soil C (e.g. Franzluebbers et al., 2000; Šantrůčková et al., 2006). Due to
232 different sample pretreatment, including duration until drying and incubation experiment, as well as
233 the different ‘local’ soil inoculi used, we consider the CryoCarb incubations of the three different
234 study areas as separate experiments.

235

236 *2.4. Geochemical parameters and C-CO₂ production rates*

238 As potential explanatory geochemical parameters we have considered dry bulk density (DBD),
 239 carbon content (%C of dry weight) and carbon to nitrogen weight ratios (C/N). In this study, we
 240 focus on the relationship between %C in samples and the corresponding C-CO₂ production in
 241 aerobic incubation experiments. An important practical reason is that %C is most widely available
 242 since it can be derived with a high degree of confidence from Elemental Analysis, but also from
 243 indirect methods such as loss-on-ignition at 550 °C. However, there are also theoretical
 244 considerations for the choice of %C. DBD is expected to be related to quantity and degree of
 245 compaction (decomposition) of SOM. However, in the permafrost layer of soils it will also co-vary
 246 with the volume of excess ground ice. C/N is a good indicator of degree of SOM decomposition in
 247 peat deposits (Kuhry and Vitt, 1996) and tundra upland soils (Ping et al., 2008). Recent soil carbon
 248 inventories in permafrost terrain have shown a clear decrease in soil C/N as a function of age/depth
 249 (e.g., Hugelius et al., 2010; Palmtag et al., 2015). However, C/N is also sensitive to original botanical
 250 composition of the peat/soil litter. In contrast, the %C of plant material is much more narrowly
 251 constrained to around 50 % of dry plant matter. For instance, based on data in Vardy et al. (2000),
 252 we can calculate a C/N range of 48.5 ± 27.9 (mean and standard deviation) in modern phytomass
 253 samples from permafrost peatlands in the Canadian Arctic (n=27) that included vascular plants,
 254 mosses and lichens. The corresponding %C range was much narrower at 47.3 ± 5.1 . An additional
 255 benefit of using %C is that it has a clear 'zero' intercept in regressions against C-CO₂ production per
 256 gram dry weight per day (i.e., at zero %C in soil samples we can expect zero C release). This is also
 257 the reason why expressing C release as a function of gram dry weight (gdw) is more straightforward
 258 than against gram C (gC). The latter would have the benefit of expressing C release directly as a
 259 function of C stock, but the relationship is complex with recent studies showing high initial C release
 260 rates per gC at low %C values (Weiss et al., 2016; Faucherre et al., 2018). In this study DBD is
 261 available for all samples, and we can also express C release as a function of soil volume (cm³). In the
 262 results we primarily show $\mu\text{gC-CO}_2$ production per gdw per day ($\mu\text{gC-CO}_2 \text{ gdw}^{-1} \text{ d}^{-1}$) as a function
 263 of %C in the sample. However, in the Supplementary Materials we also refer to regressions against
 264 C/N and C-CO₂ production rates per gC per day ($\mu\text{gC-CO}_2 \text{ gC}^{-1} \text{ d}^{-1}$) or per cm³ of soil per day ($\mu\text{gC-}$
 265 $\text{CO}_2 \text{ cm}^{-3} \text{ d}^{-1}$) against %C₂ to test the robustness of our results.

266

267 2.5. Landscape partitioning

268

269 We have investigated C-CO₂ production rates for the full datasets as well as for samples grouped
 270 into landscape unit classes that can be used for an assessment of vulnerable C pools at northern
 271 circumpolar levels. For this purpose, we have subdivided our datasets to reflect the main Gelisol
 272 suborders, non-permafrost mineral soils and Histosols recognized in the spatial layers of the
 273 NCSCD, as well as deeper Quaternary deposits for which there are separate estimates of spatial
 274 extent, depth and SOC stocks (Tarnocai et al., 2009; Strauss et al., 2013; Hugelius et al., 2014). We
 275 identify the following landscape classes: peat deposits (Histels, and some Histosols), peaty wetland
 276 deposits (mostly Histic Gelisols, peat layer <40 cm deep), mineral soils (Turbels and Orthels, and
 277 some non-permafrost mineral soils) in mountain and lowland settings, fluvial/deltaic (alluvial)
 278 deposits, and eolian/Pleistocene Yedoma deposits. Special attention is paid to the lability of SOM in
 279 Holocene peat deposits, in deeper C-enriched buried layers and cryoturbated pockets, and in
 280 Pleistocene Yedoma deposits. All main classes are represented in the PAGE21 and CryoCarb 1-
 281 Kolyma incubation experiments. The CryoCarb 2-Taymyr dataset lacks sites with eolian parent
 282 materials, whereas the CryoCarb 3-Seida dataset does not include soils formed into either alluvial or
 283 eolian deposits. Pleistocene Yedoma deposits are only represented in the CryoCarb 1-Kolyma
 284 experiment. We, therefore, focus on results from the PAGE21 and CryoCarb 1-Kolyma experiments
 285 but present the main results from the two other experiments in the Supplementary Materials. For a

286 [full overview of landscape unit class representation in each of the incubation experiments and study](#)
287 [areas, see Table S2.](#)

288 [In addition, we have applied a further subdivision of landscape unit classes in the PAGE21](#)
289 [experiment to allow a more detailed statistical analysis of the dataset and assess the role of](#)
290 [minerogenic inputs, cryoturbation and peat accumulation in SOM lability. For this purpose, the](#)
291 [eolian class is separated into actively accumulating deposits \(Adventdalen\) and Holocene soils](#)
292 [formed into Pleistocene Yedoma parent materials \(Lena Delta\); Alluvial deposits are subdivided into](#)
293 [profiles from active and pre-recent floodplains \(multiple study areas\); Mineral soils are separated](#)
294 [into active colluviation sheets \(mountain slopes on Svalbard\) and other mineral soils \(multiple study](#)
295 [areas\); Finally, for wetland deposits we discriminate between peat deposits \(fens and bogs in](#)
296 [Stordalen Mire; >40cm peat\) and peaty wetland profiles \(multiple study areas, <40 cm peat\). It](#)
297 [should be stressed that these subclasses are not specifically recognized in any circumpolar SOC](#)
298 [database and therefore of limited use for further upscaling. In all cases, SOM lability in samples of](#)
299 [deeper C-enriched buried layers and cryoturbated pockets is shown for comparative purposes.](#)

301 2.6. Statistics

302
303 Relationships between C-CO₂ production rates and geochemical parameters for all samples, as well
304 as for groupings of samples into landscape unit classes, for each incubation experiment separately,
305 are statistically analyzed using linear, polynomial and other non-linear regressions in the Microsoft
306 Excel 2010 and Past3 (Hammer et al., 2001) software packages. Regressions are considered
307 significant if $p < 0.05$. These analyses visualize SOM lability for full profiles including samples from
308 topsoil organic to mineral layers that have a wide range of DBD, %C and C/N values. In some cases,
309 replicates are not normally distributed (or even unimodal) and statistics should be interpreted with
310 caution. This is particularly the case in peatland profiles, with clusters of samples with low DBD and
311 high %C and C/N in the peat and opposite trends in samples of the underlying mineral subsoil.

312 To alleviate the issue on non-normal distributions, C-CO₂ production rates in samples as a
313 function of %C are also tested grouped into soil horizons ([PAGE21 and CryoCarb 1-Kolyma](#)
314 [experiments](#)). This approach yields classes that are much better constrained in terms of %C values.
315 Because data were still not fully normally distributed, non-parametrical Mann-Whitney tests were
316 used (Hammer et al., 2001). The data were log-transformed to reduce skewness in data distributions
317 and to reduce the influence of fractional data. [For the mineral soils in the PAGE21 incubation](#)
318 [experiment, we differentiated between the topsoil organic layer, the active layer mineral soil, the](#)
319 [permafrost layer mineral soil, and C-enriched pockets in both active layer and permafrost layer.](#)
320 [Samples from topsoil organic layer, the active layer mineral soil and the permafrost layer mineral](#)
321 [soil from profiles formed in Late Holocene loess deposits in Adventdalen \(Svalbard\) are considered](#)
322 [separately, as are the active layer peat samples from Stordalen Mire \(N Sweden\). A similar grouping](#)
323 [has been made for mineral soils in the CryoCarb 1-Kolyma experiment. In this case, Pleistocene](#)
324 [Yedoma loess samples \(both frozen and thawed\) are considered separately. Peat samples are much](#)
325 [better represented in the CryoCarb 1-Kolyma than PAGE21 experiment, and are subdivided into](#)
326 [samples from thin peat layers in the active layer of peaty wetlands \(Histic Gelisols\), as well as](#)
327 [samples from the active layer and permafrost layer of deep peat deposits \(Histels\).](#) For this approach,
328 we express C-CO₂ production rates per gC to take into account the large differences in %C among
329 the different soil horizon classes. The tests are run to evaluate null hypotheses regarding differences
330 in SOM lability between soil horizon classes, with a focus on those that are considered typical for
331 specific landscape ~~unit~~-classes (C-enriched pockets for Turbels, peat samples for Histels and loess
332 samples for Pleistocene Yedoma).

334 3. Results

335

336 *3.1. Simple geochemical indicators of SOM lability*

337

338 We first assessed the relationship between C release rates in incubation experiments and widely
339 available physico-chemical parameters in samples from soil carbon inventories carried out
340 throughout the northern permafrost region. The latter include dry bulk density (DBD), C content as a
341 percentage of dry sample weight (%C), and carbon to nitrogen weight ratios (C/N). In recent studies
342 dealing with incubation of soil samples from the northern permafrost region, %C and C/N of soil
343 samples were highlighted as best parameters to predict C release (Elberling et al., 2013; Schädel et
344 al., ~~2013~~2014). DBD was highlighted as a useful proxy in the recent synthesis of PAGE21 incubation
345 studies presented in Faucherre et al. (2018). All three parameters are significantly (anti-)correlated
346 with each other in the four different incubation experiments (Table 1 and Fig. S1). This can be
347 expected, since organically enriched topsoil samples have low DBD, high %C and high C/N values
348 compared to mineral layer soil samples. Also deeper soil samples, C-enriched through the process of
349 cryoturbation (Bockheim, 2007), have generally relatively low DBD, high %C and high C/N values
350 compared to adjacent mineral soil samples (e.g. Hugelius et al., 2010; Palmtag et al., 2015).

351

352 Table 1. R² values of cross correlations and number of samples (in brackets) between three
353 geochemical parameters ~~for all samples~~ in the PAGE21 and three CryoCarb incubation
354 experiments (all significant, p<0.05). For regression models see Figure- S1.

355

356 All three considered geochemical parameters are significantly (anti-)correlated with measured C
357 release rates in the four different incubation experiments. Lower DBD, higher %C and higher C/N
358 values are associated with higher C-CO₂ production per gdw of the samples (Table 2 and Fig. S2).
359 Of the three parameters, DBD explains most of the observed variability in C release in two
360 experiments, whereas C/N shows highest R² values in the other two experiments.

361

362 Table 2. R² values of regressions and number of samples (in brackets) between three geochemical
363 parameters and µgC-CO₂ production per gram dry weight ~~for all samples~~ in the PAGE21 and
364 ~~the~~ three CryoCarb incubation experiments (all significant, p<0.05). For regression models see
365 Figure- S2.

366

367 *3.2. Partitioning of the datasets based on landscape unit classes*

368

369 Our results show a significant relationship between µgC-CO₂ production per gdw as a function of
370 %C of the soil sample for the full datasets in each of the four incubation experiments (Table 2 and
371 Fig.- S2). However, less than 50 % of the variability is explained by this relationship, which implies
372 that it has limited usefulness to predict C release ~~based on %C of the samples only (Table 2)~~.
373 Both The experiments show a large range in µgC-CO₂ production per gdw C-release, particularly at
374 medium to high %C values. In this section we analyze whether a grouping of samples according to
375 landscape unit classes can disentangle some of the observed variability.

376

377 Figure 2 shows the ~~significant~~ relationships between C release rates and %C in the samples for
378 the ~~full-datasets~~ grouped according to major landscape unit classes in the PAGE21 (measured on day
379 343 of incubation) and CryoCarb 1-Kolyma (measured over the first four days of incubation)
380 experiments. For the sake of simplicity, we apply linear regressions with intercept zero to all classes.
These are identified by different colors and symbols that have been consistently used in Figs. 2-3 and

381 S3-S5. The regression for the full data set is provided as reference (dotted lines), but it should be
382 noted that its slope is partly determined by the number of samples in each of the recognized
383 landscape units.

384
385 Figure 2. $\mu\text{gC-CO}_2$ production per gram dry weight as a function of %C of the sample for the full
386 datasets in the (a) PAGE21 (top panel) and (b) CryoCarb 1-Kolyma (lower panel) incubation
387 experiments (both regressions significant, $p < 0.05$).

388 Figure 32. $\mu\text{gC-CO}_2$ production per gram dry weight as a function of %C of the sample for the full
389 datasets and different landscape classes in the longer-term PAGE21 (a, top panel) and short-
390 term CryoCarb 1-Kolyma (b, lower panel) incubation experiments: All samples (dotted grey
391 lines; Alluvial class (red line and diamonds); Eolian class (blue line and triangles); Mineral class
392 (brown line and squares); Peaty wetland class (dark green line and circles); Peatland class (light
393 green line and circles). All regressions significant, $p < 0.05$, except for the PAGE21 peatland
394 class (n.s.).

395
396 A first observation is that C release rates per gdw are c. 15 times lower in the longer-term
397 PAGE21 experiment compared to the short-term CryoCarb 1-Kolyma experiment. In the PAGE21
398 dataset (Fig. 3a2a), the soils developed into alluvial and eolian deposits and in peaty wetlands all
399 show similar and relatively high SOM lability. Mineral soils show intermediate values, whereas the
400 peat deposits display low SOM lability (when considering %C values). All regressions are
401 significant, except for 'peat deposits' due to very high variability in three surface peat samples (but
402 see Fig. 4d3d). In the CryoCarb 1-Kolyma data set (Fig. 3b2b), alluvial and eolian soils/deposits
403 show the highest SOM lability, followed by mineral soils. In this case, peaty wetlands show a
404 slightly lower lability than mineral soils/deposits but still considerably higher than peatlands. This
405 clear dichotomy in the SOM lability of mineral soils (including peaty wetlands) and peat deposits is
406 also apparent from the CryoCarb 2-Taymyr and CryoCarb 3-Seida results even though not all
407 landscape classes are represented in those experiments (Fig. S3). The explanatory power of the
408 regressions (R^2 values) in the peatland class is generally lower than that in the mineral soil/deposit
409 classes. These statistics are, however, greatly improved when removing the surface peat samples
410 from the analyses (not shown), which display very high variability.

411 Linear regression analyses between C- CO_2 production per gdw and C/N ratios for all four
412 experiments (Fig. S4) show small deviations from the above patterns but generally maintain the clear
413 difference between 'peat deposits' and the remaining landscape units. However, C- CO_2 production
414 was similar in peat deposits and mineral soils/deposits at low peat deposits with low C/N values
415 (≤ 20) seem to decompose at similar rates as SOM in mineral soils and deposits with similar C/N
416 ratios. R^2 values for the landscape classes are generally lower than in regressions against %C and
417 regression lines at low C release tend to converge to C/N values of 8-12, which are typical for
418 microbial decomposer biomass suggesting only slow internal cycling of remaining SOM
419 (Zechmeister-Boltenstern et al., 2015).

420 The PAGE21 dataset with C- CO_2 production rates expressed per gC as a function of %C of the
421 soil sample also shows similar results, however, with generally lower R^2 and sometimes non-
422 significant regressions (Fig. S5a). The same patterns are also noted when expressing C release as a
423 function of soil volume (cm^3), however, R^2 values are generally even lower and more often non-
424 significant (Fig. S5b).

425
426 *3.3. Further subdivision of landscape unit classes in the PAGE21 dataset*

427

428 ~~In Figure 43a-dc, presents SOM lability in a further subdivision of the mineral soil/deposit~~
429 ~~landscape unit classes in the PAGE21 dataset. We have compared profiles with active~~
430 ~~accumulation/movement in eolian, alluvial and colluvial settings, with Holocene soils developed into~~
431 ~~older eolian, alluvial or other mineral parent materials, respectively. In each of these comparisons,~~
432 ~~we specifically identify samples from deeper C-enriched buried layers and cryoturbated pockets.~~
433 ~~have been further subdivided and different functions (second order polynomial or exponential)~~
434 ~~providing better fits have been applied. The eolian class is subdivided into actively accumulating~~
435 ~~deposits (Adventdalen) and Holocene soils formed into Pleistocene Yedoma parent materials (Lena~~
436 ~~Delta), and specifically identifies buried C-enriched samples (Fig. 4a3a). Alluvial deposits are~~
437 ~~separated into profiles from active and pre-recent floodplains (multiple study areas), again separating~~
438 ~~samples from deeper C-enriched buried layers and cryoturbated pockets (Fig. 4b3b). Mineral soils are~~
439 ~~separated into active colluviation sheets (mountain slopes on Svalbard) and other mineral soils~~
440 ~~(multiple study areas), highlighting the one buried C-enriched sample found in this class (Fig. 4c3c).~~
441 Generally speaking, a second order polynomial (intercept zero) provides the best fit and has been
442 applied for the sake of uniformity to all described subclasses. All these ~~three~~ datasets have in
443 common that the subclasses with active surface accumulation/movement have topsoil samples that
444 show relatively low C content due to the continuous admixture of minerogenic materials. At the
445 same time, these all show the highest C-CO₂ production per gdw (when considering %C).
446 Furthermore, the second order polynomial regressions of all subclasses (except for buried C-enriched
447 samples) suggest that the topsoil samples are particularly labile suggesting the presence of a
448 ~~‘fast’ more degradable~~ SOM pool in the recently deposited plant litter. Deeper C-enriched material
449 shows relatively low lability and does not show rapidly increasing lability at higher %C values.

450 Figure ~~4d-3d~~ compares the SOM lability in ~~peat fen and bog~~ deposits (~~fens and bogs in~~ Stordalen
451 Mire) and peaty wetland profiles (multiple study areas), adding for comparison the results from the
452 previously described deeper C-enriched buried layers and cryoturbated pockets in mineral soils (see
453 Figs. ~~4a3a-c~~). In this case, exponential functions best describe observed trends ~~and, pointing~~
454 ~~to indicate~~ very high lability of surface peat(y) samples. The thin peat layers in peaty wetlands have
455 relatively low %C values pointing to admixture of minerogenic materials. The SOM in these profiles
456 show relatively high C-CO₂ production per gdw compared to ‘true’ peat samples (when considering
457 %C). Compared to the non-significant linear regression for all peat samples shown in Fig. ~~3a2a~~,
458 exponential regressions for the peatland class as a whole as well as for fens and bogs separately are
459 statistically significant. Particularly in fen peat, this regression is able to capture some very high C
460 release values of two surface peat samples (corresponding to graminoid-derived plant litter). Deeper
461 C-enriched material in mineral soils displays only slightly higher SOM lability compared to the
462 mineral subsoil underlying peat deposits. It is important to bear in mind that the total number of peat
463 samples from Stordalen Mire is limited (n=13) and that results cannot be compared directly to
464 adjacent mineral soil profiles because field sampling in that particular study area focused solely on
465 the peatland area.

466

467 Figure 43. $\mu\text{gC-CO}_2$ production per gram dry weight as a function of %C of the sample for different
468 landscape classes and their subdivisions in the PAGE21 incubation experiment. (a) Eolian class
469 separated into actively accumulating deposit (light blue), Holocene soil formation into
470 Pleistocene Yedoma parent materials (dark blue) and buried C-enriched samples (pink); (b)
471 Alluvial class separated into active floodplain (rose), Holocene soil formation into pre-recent
472 floodplain deposits (red) and buried C-enriched samples (pink); (c) Mineral class separated into
473 active colluviation sheet (light brown), other mineral soils (dark brown) and ~~the one~~ buried C-
474 enriched samples (pink); (d) ~~W~~wetland class separated into wetlands with thin peat layers
475 (green), fens (light green) and bogs (dark green) with deep peat deposits and, for comparison,

476 buried C-enriched samples in mineral soils (pink). The hatched line represents the regression for
477 all ~~true~~ peatland samples (fens and bogs) together. C-release from one surface peat sample
478 (green-orange) in the margin of a peatland is also indicated, but not included in the regressions.
479 All regressions are significant ($p < 0.05$).

480

481 3.4. C-enriched cryoturbated and Pleistocene Yedoma samples in the CryoCarb 1-Kolyma dataset

482

483 In the PAGE21 incubation each collected profile included only one sample from the mineral soil in
484 the middle of the active layer and one sample from the upper permafrost layer. Thus, the selection of
485 samples was based on depth-specific criteria. As a result, the number of samples from deeper C-
486 enriched buried layers and cryoturbated pockets is limited ($n=13$). In the CryoCarb 1-Kolyma
487 experiment samples from entire profiles were incubated and the number of deeper C-enriched
488 samples in the mineral soil horizons is much larger. Figure ~~5a-4a~~ compares the C-CO₂ production per
489 gdw from organically-enriched topsoil and mineral soil samples not affected by C-enrichment with
490 that in deeper C-enriched cryoturbated samples in tundra ~~upland~~ profiles. For the sake of clarity, only
491 those cryoturbated samples which are C-enriched by at least twice the adjacent mineral soil %C
492 background values are included ($n=22$). It should be emphasized that the actual absolute %C values
493 for the C-enriched samples and mineral soil samples not affected by C-enrichment can vary between
494 study areas and profiles, among others due to differences in soil texture (Palmtag and Kuhry, 2018).
495 The results from this much more narrowly defined dataset are similar to those presented for the
496 PAGE21 experiment, i.e. SOM in deeper C-enriched cryoturbated samples is less labile than in
497 organically-enriched topsoil samples with similar %C.

498 The PAGE21 experiment does not include any samples from Pleistocene Yedoma deposits. In
499 contrast, the CryoCarb 1-Kolyma dataset ~~includes-has~~ samples from two Yedoma exposures along
500 river and thermokarst lake margins. The material was collected from perennially frozen Yedoma
501 deposit as well as from thawed out sections of the exposures. C-release from these samples are
502 presented in Figure 4b, which for comparison also shows samples from Holocene lowland soils,
503 mineral subsoil samples beneath peat deposits and deeper C-enriched cryoturbated samples. The C-
504 CO₂ production per gdw of Pleistocene Yedoma is lower than that of Holocene lowland soils, but
505 somewhat higher than that of mineral subsoil beneath peat and deeper C-enriched material (when
506 considering %C). Furthermore, the SOM lability of thawed out deposits is somewhat lower than that
507 of the intact permafrost Yedoma material.

508

509 Figure 4. $\mu\text{gC-CO}_2$ production per gram dry weight as a function of %C of the sample in the
510 CryoCarb 1-Kolyma incubation experiment for (a) Deeper C-enriched samples (pink line and
511 triangles), compared to samples of organically enriched topsoil and mineral soil not affected by
512 C-enrichment in all tundra profiles (blue line and triangles, showing lower part of regression
513 line), and for (b) Perennially frozen Pleistocene Yedoma samples (black line and triangles) and
514 thawed out Pleistocene Yedoma samples (red line and triangles), compared to samples of
515 organically enriched topsoil and mineral soil not affected by C-enrichment in Holocene lowland
516 profiles (blue line and triangles, showing start of regression line), mineral subsoil samples
517 beneath peat deposits (green line and circles, showing start of regression line) and buried C-
518 enriched samples (pink line and triangles, showing start of regression line). All regressions
519 (power fit) are significant ($p < 0.05$).

520

521 3.5. Relative lability ranking of SOM landscape unit classes

522

523 Table 3a shows the slopes of the linear regressions (intercept zero) between C-CO₂ production per
524 gdw and %C of samples for the different landscape unit classes in all four incubation experiments.
525 From these results it is clear that results from the four experiments cannot be compared directly in
526 quantitative terms. To facilitate comparison across experiments ~~the results were therefore~~ normalized
527 to the lowland mineral soil class, which consistently showed intermediate SOM liabilities. Table 3b
528 shows the normalized regression slopes (with the slope for mineral soils set to 1), and their mean and
529 standard deviation (when the landscape class is represented in more than one incubation experiment).
530 This approach confirms the previous results that peat deposits and deeper C-enriched samples in
531 mineral soils consistently show very low relative liability, whereas areas with recent mineral sediment
532 accumulation (~~e.g. in active floodplains and~~ recent eolian deposits) display generally somewhat
533 higher SOM liability (when considering %C). Pleistocene Yedoma deposits, only represented in one
534 incubation experiment, also display relative low SOM liability.

535

536 Table 3. (a) Slopes of linear regressions (intercept zero) between %C and C-CO₂ production per gdw
537 in samples of the different landscape classes in the four experiments; (b) Normalized slopes of
538 linear regressions between %C and C-CO₂ production per gdw for samples in the different
539 landscape classes in the four experiments (slope of mineral soils in lowland settings set to 1).
540 Abbreviations: 'Pt' = peat deposits (Histels/Histosols), excluding two surface graminoid litter
541 samples (PAGE21, Stordalen Mire); 'Min/CE' = C-enriched pockets in cryoturbated soils
542 (Turbels); 'Min Mtn' = mineral soils in mountain settings; 'Min Pty' = peaty wetlands (mineral
543 soils with histic horizon); 'Min Lowl' = mineral soils in lowland settings; 'Alluv' = recent alluvial
544 deposits and Holocene soils formed in alluvial deposits; 'Eol' = recent eolian deposits; 'Pl Yed' =
545 Pleistocene Yedoma deposits.

546

547 3.6. SOM liability based on soil horizon criteria

548

549 We also tested SOM liability in samples grouped according to soil horizon criteria ([PAGE21 and](#)
550 [CryoCarb 1-Kolyma experiments](#)), with special attention to those horizon classes that can be linked
551 to the specific landscape units ~~that showing~~ low relative SOM liability (C-enriched pockets for
552 Turbels, peat samples for Histels and loess samples for Pleistocene Yedoma). This approach yielded
553 classes with data distributions that are much better constrained in terms of %C values.

554 ~~For the mineral soils in the PAGE21 incubation experiment, we differentiated between the~~
555 ~~topsoil organic layer, the active layer mineral soil, the permafrost layer mineral soil, and C-enriched~~
556 ~~pockets in both active layer and permafrost layer. Samples from topsoil organic layer, the active~~
557 ~~layer mineral soil and the permafrost layer mineral soil from profiles formed in Late Holocene loess~~
558 ~~deposits in Adventdalen (Svalbard) are considered separately, as are the active layer peat samples~~
559 ~~from Stordalen Mire (N-Sweden). A similar grouping has been made for mineral soils in the~~
560 ~~CryoCarb 1-Kolyma experiment. In this case, Pleistocene Yedoma loess samples (both frozen and~~
561 ~~thawed) are considered separately. Peat samples are much better represented in the CryoCarb 1-~~
562 ~~Kolyma than PAGE21 experiment, and are subdivided into samples from thin peat layers in the~~
563 ~~active layer of peaty wetlands (Histic Gelisols), as well as samples from the active layer and~~
564 ~~permafrost layer of deep peat deposits (Histels).~~

565 In this analysis we focus on C-CO₂ production per gC to take into account large differences in
566 %C between soil horizon classes (see Fig. S6). The main difference between the two experiments is
567 the much lower %C values of the topsoil organic class in the PAGE21 incubation, which can be
568 explained by a greater surface admixture of minerogenic material in alluvial (Lena Delta), eolian and
569 mountainous areas (Svalbard). In contrast, the predominant lowland setting of the CryoCarb 1-
570 Kolyma study area is characterized by soils with thicker, more C-rich, topsoil organic layers.

571 Figure 65 shows C-CO₂ production per gC in the soil horizon groups of the longer term
572 PAGE21 and short-term CryoCarb 1-Kolyma experiments. Results of the Mann-Whitney paired tests
573 for both these experiments are shown in Table 4. PAGE21 classes show fewer statistically significant
574 differences than in the CryoCarb 1-Kolyma experiment, which can at least partly be ascribed to
575 smaller sample sizes. The number of samples in the PAGE21 incubation for C-enriched pockets in
576 the active layer (n=3) and for peat (n=6) are particularly low.

577

578 Figure 65. $\mu\text{gC-CO}_2$ production per gram carbon in samples of (a) the PAGE21 and (b) the
579 CryoCarb 1-Kolyma incubation experiments, grouped according to soil horizon criteria.
580 Abbreviations: AL-OL = Active layer topsoil organics; AL-Min = Active layer mineral; AL-Ce
581 = Active layer C-enriched; P-Min = Permafrost layer mineral; P-Ce = Permafrost layer C-
582 enriched; AL-Pty = Active layer thin peat (CryoCarb 1-Kolyma experiment only); AL-Pt =
583 Active layer peat; P-Pt = Permafrost layer peat (CryoCarb 1-Kolyma experiment only); AL-Lss
584 OL = Active layer topsoil organics in Late Holocene loess deposits (PAGE21 experiment only);
585 AL-Lss Min = Active layer mineral in Late Holocene loess deposits (PAGE21 experiment only);
586 P-Lss Min = Permafrost layer mineral in Late Holocene loess deposits (PAGE21 experiment
587 only); **PFr**-Yed = Permafrost Pleistocene Yedoma deposits (CryoCarb 1-Kolyma experiment
588 only); Th-Yed = Thawed out Pleistocene Yedoma deposits (CryoCarb 1-Kolyma experiment
589 only). Box-whisker plots show mean and standard deviation (in red) and median, first and third
590 quartiles and min/max values (in black), for the different soil horizon groups.

591

592 Table 4. p Values of Mann-Whitney paired tests of $\mu\text{gC-CO}_2$ production per gram carbon for soil
593 horizon groups in (a) the PAGE21 and (b) the CryoCarb 1-Kolyma incubation experiments.
594 Abbreviations as in Figure- 65. Differences are considered significant when $p < 0.05$. Yellow
595 denotes significant differences ($p < 0.05$).

596

597 ~~The~~ C release rates in topsoil organic samples from ~~the~~ actively accumulating Holocene loess
598 soils are significantly higher than those in topsoil organic samples from the remaining PAGE21
599 mineral soils (Fig. 6a-5a and Table 4a). Both topsoil organic classes show significantly higher rates
600 than all mineral soil and peat classes. Peat samples have the lowest mean and median C release rates
601 from all these classes but only the rates from permafrost layer mineral soil and C-enriched pocket
602 samples are significantly higher. Both mean and median C release rates from active layer and
603 permafrost layer C-enriched pockets are somewhat lower (but not significantly different) than those
604 from adjacent, non C-enriched, mineral soil samples.

605 C release rates in the soil horizon classes from the CryoCarb 1-Kolyma experiment show
606 similarities, but also some differences to those observed in the PAGE21 experiment. Absolute C
607 release rates per gC are more than an order of magnitude higher in the CryoCarb 1-Kolyma
608 experiment (measured as a mean release over the first four days of incubation) compared to those in
609 the PAGE21 experiment (measured at-on day 343 of incubation). Another important difference is
610 that C release rates per gC in the short-term CryoCarb 1-Kolyma incubation do not differ
611 significantly between the topsoil organic class and the active layer and permafrost layer mineral soil
612 classes, which we ascribe to the presence of a highly labile C pool (e.g. DOC, plant roots) in the
613 mineral soil layers that is quickly decomposed (see Weiss et al., 2016; Faucherre et al., 2018).
614 However, rates from active layer and permafrost layer C-enriched pockets are significantly lower
615 than those from adjacent, non C-enriched, mineral soil samples. Both active layer and permafrost
616 layer peat samples show significantly lower C release rates than all other classes, with active layer
617 peat samples having significantly higher rates than permafrost layer peat samples. Samples from the
618 Pleistocene Yedoma loess ‘frozen’ and ‘thawed’ classes display significantly lower C release rates
619 per gC than those in the topsoil organic layer, active layer and permafrost layer mineral soil classes,

620 but significantly higher rates than those in the peat classes. The two Yedoma classes do not differ
621 significantly from each other, the active layer and permafrost layer C-enriched pocket classes, nor the
622 peaty wetland class.

623

624 4. Discussion

625

626 The analysis and comparison of results in the PAGE21 and CryoCarb 1-Kolyma incubations show
627 consistent trends in C-CO₂ production rates as a function of simple soil geochemical parameters in
628 both the full datasets as well as in the grouping of samples according to landscape classes. However,
629 it is not possible to directly compare these two very different laboratory experiments quantitatively.
630 The varying field collection techniques, field storage, transport and laboratory storage, pretreatment,
631 experimental setup and time of measurement after start of incubations have a clear effect on the
632 magnitude of the observed C-CO₂ production rates. The same methods were applied to all samples
633 from all study areas in the PAGE21 experiment, but these differed markedly from those applied in
634 the CryoCarb setup and even between the three individual CryoCarb experiments (e.g., addition of
635 different 'local' microbial decomposer inoculi to rewetted samples).

636 In quantitative terms, C-CO₂ production rates per gdw measured over the first 4 days in the
637 CryoCarb 1-Kolyma samples incubated at 12 °C are about 15 times higher than those [measured](#) after
638 about one year in the PAGE21 samples incubated at 5 °C (see Fig. 2). Similarly, C-CO₂ production
639 rates per gC are also more than an order of magnitude higher in the short-term CryoCarb-Kolyma 1
640 than the longer term PAGE21 incubation (see Fig. [65](#)). Upper permafrost mineral soil samples (<3
641 %C) from Kylatyk in NE Siberia, incubated at 2 °C directly after field collection and thawing
642 (measurement after 20-30 hr, following 3 days of pre-incubation), show median C release rates of c.
643 750 µgC-CO₂ gC⁻¹ d⁻¹ (Weiss et al., 2016), compared to c. 1750 µgC-CO₂ gC⁻¹ d⁻¹ in the same class
644 of CryoCarb 1-Kolyma samples. Median C release rates in upper permafrost mineral soil samples of
645 the PAGE21 experiment (Faucherre et al., 2018) decrease from c. 170 on day 8 to c. 35 µgC-CO₂
646 gC⁻¹ d⁻¹ on day 343 since start of incubation. It is obvious from these results that there is a rapid
647 decline in C release rates over time of incubation. Longer incubation experiments (up to 12 years)
648 have shown that the overall rate of C loss decreases almost exponentially over time (Elberling et al.,
649 2013). However, even when laboratory incubation setups and time of measurement are similar, large
650 differences can occur in C release rates. For instance, peat samples in the CryoCarb 1-Kolyma
651 incubation display about twice the C-CO₂ production rates per gdw than those observed in the
652 CryoCarb 3-Seida incubation (Figs. [3b-2b](#) and S3b).

653 Nonetheless, a comparison of C-CO₂ production rates per gdw for landscape unit classes in
654 terms of relative SOM lability provided useful and robust results. These classes were implemented to
655 allow upscaling of results to the northern permafrost region. They reflect main Gelisol (and non-
656 Gelisol) soil suborders and deeper Quaternary deposits to permit direct comparison with the size and
657 geographic distribution of these different SOC pools (Tarnocai et al., 2009; Hugelius et al., 2014).
658 Samples from mineral soil profiles, including wetland deposits with a thin peat(y) surface layer,
659 display high relative SOM lability compared to peat deposits, deep C-enriched buried or cryoturbated
660 samples and Pleistocene Yedoma deposits (when considering %C of the incubated sample). These
661 results are confirmed by the more stringent statistical analysis of samples grouped into soil horizon
662 classes. Peat deposit, C-enriched pocket and Yedoma deposit samples show significantly lower C-
663 CO₂ production rates per gC than topsoil organics and mineral layer samples (Cryo-Carb-1-Kolyma
664 experiment). The same trends are observed in the incubation experiment of upper permafrost samples
665 from Kytalyk, reported by Weiss et al. (2016). C-enriched pockets (3-10 %C) showed lower C-CO₂
666 production rates per gC than mineral soil samples (<3 %C), while a buried peat sample (c. 40 %C)
667 displayed a very low C-CO₂ production rate per gC. The PAGE21 experiment also revealed that peat

668 samples mineralized a smaller fraction of C over the one year of incubation compared to mineral soil
669 samples (Faucherre et al., 2018).

670 A further subdivision of landscape classes and more careful analysis of incubation results in the
671 PAGE21 experiment provide additional useful insights. For example, separation of eolian deposits
672 into actively accumulating deposits during the Late Holocene (Adventdalen) and Holocene soils
673 formed into Pleistocene Yedoma parent materials (Lena Delta) showed clear differences in C release
674 rates per gdw (when considering %C), with the former displaying a higher SOM lability in topsoil
675 organic samples (see Fig. 4a3a). The topsoil organic samples from the actively accumulating eolian
676 deposits in Adventdalen also displayed significantly higher C release rates per gC than all other
677 topsoil organic, mineral layer and peat(y) horizon classes (see Table 4a). Separation of alluvial
678 deposits into active floodplain deposits and Holocene soils formed in pre-recent river terraces and of
679 mineral soils into active colluviation sheets (mountain slopes on Svalbard) and other mineral soils
680 (~~multiple study areas~~) showed similar trends in SOM lability (see Fig. 4b3b-c). These results suggest
681 that admixture of minerogenic material in topsoil organics of actively accumulating eolian, alluvial
682 and colluvial deposits promotes SOM decomposition. Peaty wetland deposits display much higher C
683 release rates per gdw (when considering %C) than peatland deposits (see Fig. 4d3d). These two
684 landscape classes are poorly represented in the PAGE21 experiment, but a statistical test of C release
685 rates per gC in these peat(y) soil horizon classes of the CryoCarb 1-Kolyma incubation confirms this
686 difference (see Table 4b). This is interesting because even though wetlands with a thin peat layer do
687 not have particularly high C stocks, they can be important sources of methane (CH₄) to the
688 atmosphere (Olefeldt et al., 2013). These further subdivisions into landscape subclasses are of
689 limited use for upscaling purposes because they are not considered explicitly in any available
690 geographic database for the northern permafrost region.

691 The implementation of landscape classes (and their subdivisions) in the PAGE21 and CryoCarb
692 incubation experiments have greatly constrained variation in C release rates compared to the full
693 datasets. However, much within-class variability remains and there is a need to further investigate
694 the sources of this variability. Important additional soil and environmental factors such as microbial
695 community, moisture, texture, pH, redox potential, etc. were not available for the (full) PAGE21 and
696 CryoCarb datasets and could, therefore, not be tested. We conclude that additional research is needed
697 to further constrain observed SOM lability across the northern permafrost region and within the
698 classes proposed here.

699 The relatively low lability in the peatland class is surprising. The low DBD, high %C and high
700 C/N of peat are normally associated with a relatively low degree of decomposition. This, in turn, is
701 the result of environmental factors such as anaerobic and/or permafrost conditions that largely inhibit
702 SOM decay (Davidson and Janssens, 2006). One could expect that this less decomposed material
703 would show high lability following thawing and warming, but our results point to the opposite. This
704 is particularly surprising when considering the setup of the CryoCarb experiments, in which a slush
705 of rewetted material inoculated with microbial decomposers was incubated at 12 °C. ~~The~~ Although
706 the CryoCarb experiments are very short assays (4 days), ~~but~~ the longer term PAGE21 incubation
707 data experiment (measured after roughly one year) provides similar results.

708 In the case of peat deposits, it should be considered if this low decomposability is an evolved
709 'biochemical trait' in peat-forming species that maintains their favored habitat, similar to the role of
710 *Sphagnum* anatomy (hyaline cells), physiology (acidification) and cell wall chemistry (phenolic
711 compounds) in sustaining moist and acid surface conditions, and inhibiting peat decomposition
712 (Clymo and Hayward, 1982). Furthermore, the generally high C/N ratios of peat provide a poor
713 substrate quality to the decomposer community (Bader et al., 2018). Diáková et al. (2016) reported
714 low microbial biomass in subarctic peat deposits of the Seida study area (Northeast European
715 Russia).

716 Permafrost degradation in peatlands can result in two opposite pathways, one resulting in surface
717 collapse and an increase in soil moisture (particularly mimicked in the CryoCarb incubation setup)
718 and another one resulting in drainage, drying and accelerated C losses, not the least due to a higher
719 incidence of peat fires (Kuhry, 1994).

720 Our results on the low lability of peat deposits can be compared to the findings of Schädel et al.
721 (2014) in their assessment of SOM decomposability in the northern permafrost region. That study
722 recognized a group of organic soil samples (>20% initial C), ranging in depth between 0 and 120 cm.
723 We consider that this group will include both topsoil organic samples as well as deeper peat deposits.
724 In the Schädel et al. (2014) study, this group showed the largest range in decomposability, with some
725 samples showing high potential C losses, whereas deeper organic samples were less likely to respire
726 large amounts of C. We suggest, therefore, that both studies might show the same trends.

727 In our incubation experiments, SOM from deeper C-enriched buried layers and cryoturbated
728 pockets show relatively low lability when compared to organic-rich topsoil samples. These results
729 are corroborated by Čapek ~~Čapek~~-et al. (2015) and Gentsch et al. (2015b), who report low
730 bioavailability of SOM in subducted horizons of Lower Kolyma soils (NE Siberia). The reason why
731 this relatively undecomposed material displays low lability remains unclear. One reason could be
732 that the decomposer community needs time to adapt to the new environmental conditions following
733 thawing/warming, another one that there is a simple mismatch between the microbial community
734 adapted to decompose relatively undecomposed organic material and the physico-chemical
735 environment (e.g., higher bulk density) prevailing in (thawed out) deeper soil horizons (Gittel et al.,
736 2013; Schnecker et al., 2014). Kaiser et al. (2007) and Čapek ~~Čapek~~-et al. (2015) reported low
737 microbial biomass in deeper C-enriched soil samples.

738 These results pose interesting questions regarding the role of organic aggregates and organo-
739 mineral associations for SOM lability (e.g. ~~Kaiser et al., 2007~~; Gentsch et al., 2018). On the one
740 hand, our samples from topsoil organic horizons with active minerogenic inputs in eolian, alluvial
741 and colluvial settings display (very) high C release rates, whereas deeper C-enriched soil materials
742 show low decomposability. The underlying soil physico-chemical and microbial processes require
743 urgent attention in order to better constrain C release rates from soils and deposits in the northern
744 permafrost region.

745 ~~To these two categories of samples can be added~~ Pleistocene Yedoma deposits, represented in
746 the CryoCarb 1-Kolyma incubation experiment, also display low relative SOM lability, which
747 despite incorporation of relative fresh plant root material caused by syngenetic permafrost
748 aggradation, also display low relative SOM lability. These results are corroborated by results from
749 Schädel et al. (2014) for their group of deep mineral samples (with Yedoma provenance).

750 An important consideration is if the consistent differences in relative SOM lability of landscape
751 and soil horizon classes observed in our incubation experiments will be maintained over periods of
752 decades to centuries of projected warming and thawing. Very short-term incubations, such as in the
753 CryoCarb setup (four days), might register the initial decomposition of highly labile SOM
754 components, such as microbial necromass, simple molecules (e.g., sugars or amino acids), low
755 molecular-weight DOC, etc., or might not provide enough time for an adaptation of the microbial
756 decomposer community to new environmental settings (Weiss et al., 2016; Weiss and Kaal, 2018).
757 On the other hand, in longer incubation experiments such as in the PAGE21 experiment (one year),
758 the conditions in the incubated samples become gradually more artificial compared to field
759 conditions. Specifically, microbes in long-term incubations become increasingly C limited, as no
760 new C input by plants occur, whereas inorganic nutrients, such as nitrate or ammonium accumulate
761 to unphysiological levels. Care, therefore, should be taken when extrapolating our results over longer
762 time frames if no corroborating field evidence for longer term decay rates can be obtained (e.g.
763 Kuhry and Vitt, 1996; Schuur et al., 2009).

764

765 5. Conclusions

766

767 The PAGE21 and CryoCarb incubation experiments confirm results from previous studies that
768 simple geochemical parameters such as DBD, %C and C/N can provide a good indication of SOM
769 lability in soils and deposits of the northern permafrost region (Elberling et al., 2013; Schädel et al.,
770 [2013](#)[2014](#); Faucherre et al., 2018.). In our analyses we have focused on %C of the sample since it is
771 the most widely available of the three investigated geochemical parameters. Furthermore, %C is less
772 sensitive than C/N to botanical origin of the plant litter and, in contrast to DBD, not dependent on
773 ground compaction or volume of excess ground ice.

774 When considering the full datasets of the four experiments, our regressions of C release as a
775 function of %C were statistically significant but explained less than 50 % of the observed variability.
776 Subsequently, we investigated whether a further division of samples into predefined landscape unit
777 classes would better constrain the observed relationships. In defining these classes, we applied a
778 scheme that could easily be used for spatial upscaling to northern circumpolar levels. We adopted the
779 main Gelisol suborders (Histels, Turbels and Orthels), non-permafrost Histosols and mineral soils,
780 and types of deeper Quaternary (deltaic/floodplain and eolian/Yedoma) deposits used in the NCSCD
781 and related products to estimate the total SOC pool in the northern permafrost region (Tarnocai et al.,
782 2009; Strauss et al., 2013; Hugelius et al., 2014). We conclude that these landscape classes better
783 constrain observed variability in the relationships and that the relative SOM lability rankings of these
784 classes were consistent among all four incubation experiments, for both regressions against %C and
785 C/N (all four experiments), and for regressions of %C against different units of C-CO₂ production
786 *'per gram dry weight'*, *'per gram C'* and *'per cm³'* (PAGE21 dataset). Our results based on full
787 profiles indicate that C-CO₂ production rates per gdw decrease in the order Late Holocene eolian >
788 alluvial and mineral ~~upland~~ (including peaty wetlands) > Pleistocene Yedoma > C-enriched pockets
789 > peat, with lowest C release rates observed in peat deposits (when considering %C). These results
790 are corroborated by statistical analysis of C release rates per gC for samples grouped according to
791 soil horizon criteria (PAGE21 and CryoCarb 1-Kolyma datasets).

792 An important conclusion from these results is that purportedly more undecomposed SOM, such
793 as in peat deposits (Histels and Histosols), C-enriched cryoturbated samples (Turbels), and
794 Pleistocene Yedoma deposits, does not seem to imply higher SOM lability. These three SOC pools,
795 [which](#) together represent ≥50 % of the reported SOC storage in the northern permafrost region
796 (Hugelius et al., 2014; Palmtag and Kuhry, 2018), [display relatively low rates of C release](#).
797 Consequently, there is an urgent need for further research to understand these results in order to
798 better constrain the thawing permafrost carbon feedback on global warming.

799

800 6. Data availability

801

802 The soil geochemical data and incubation results presented in this paper are available upon request
803 from PK (peter.kuhry@natgeo.su.se). For full PAGE21 incubation data, please contact BE
804 (be@ign.ku.dk). For full CryoCarb incubation data, please contact JB (jiri.barta@prf.jcu.cz).

805

806 7. Author contribution

807

808 PK developed the initial concept for the study. All authors contributed with the collection of soil
809 profiles at various sites. The PAGE21 incubation experiment was planned and conducted at
810 CENPERM (University of Copenhagen) by SF, [CJJ](#) and BE, whereas the CryoCARB incubation
811 experiments were carried out at the University of South Bohemia (Ceske Budejovice) under

812 guidance of HS and JB. PK performed all statistical analyses, in cooperation with GH. All co-authors
813 contributed to the writing of the manuscript, including its discussion section.

814

815 8. Competing interests

816

817 The authors declare that they have no conflict of interest.

818

819 9. Acknowledgments

820

821 Collection and laboratory analyses for Svalbard (Adventdalen and Ny Ålesund), Stordalen Mire and
822 Lena Delta samples were supported by the EU-FP7 PAGE21 project (grant agreement no 282700).
823 Lower Kolyma and Taymyr Peninsula samples were collected and incubated in the framework of the
824 ESF-CryoCarb project, with support from the Swedish Research Council (VR to Kuhry), the
825 Austrian Science Fund (FWF I370-B17 to Richter), the Czech Science Foundation (Project 16-
826 18453S to Barta) and the Czech Soil-Water Research Infrastructure (MEYS CZ grants LM2015075
827 and EF16-013/0001782 to Šantrůčková). Seida samples were originally collected in the framework
828 of the EU-FP6 Carbo-North project (contract 036993). Gustaf Hugelius acknowledges a Swedish
829 Research Council Marie Skłodowska Curie International Career Grant. [We thank Christian Jungner](#)
830 [Jørgensen \(University of Copenhagen\) for guidance and assistance in the PAGE21 incubation](#)
831 [experiment.](#) Kateřina Diaková is acknowledged for the collection of the soil inoculi in Seida. The
832 Seida samples were subsequently incubated at the University of South Bohemia. We are most
833 grateful to Nikolai Lashchinskiy (Siberian Branch of the Russian Academy of Sciences,
834 Novosibirsk) and Nikolaos Lampiris, Juri Palmtag, Nathalie Pluchon, Justine Ramage, Matthias
835 Siewert and Martin Wik (all Stockholm University), for help in sample collection. We would also
836 like to thank Magarethe Watzka (University of Vienna) for elemental analyses of soil samples.
837 Zhanna Kuhrij is acknowledged for the preparation of Figures [6-5](#) and [S6](#). [We thank two anonymous](#)
838 [reviewers for their constructive comments on the manuscript.](#)

839

840 10. References

841

- 842 Bader, C., Müller, M., Schulin, R., and Leifeld, J.: Peat decomposability in managed organic soils in
843 relation to land use, organic matter composition and temperature, *Biogeosciences* 15, 703-719,
844 <https://doi.org/10.5194/bg-15-703-2018>, 2018.
- 845 [Birch, H. F.: The effect of soil drying on humus decomposition and nitrogen availability, *Plant and*](#)
846 [Soil, 10, 9-31, 1958.](#)
- 847 [Biskaborn, B. K., Smith, S. L., Noetzli, J., Matthes, H., Vieira, G., Streletskiy, D. A., Schoeneich, P.,](#)
848 [Romanovsky, V. E., Lewkowicz, A. G., Abramov, A., Allard, M., Boike, J., Cable, W. L.,](#)
849 [Christiansen, H. H., Delaloye, R., Diekmann, B., Drozdov, D., Etzelmüller, B., Grosse, G.,](#)
850 [Guglielmin, M., Ingeman-Nielsen, T., Isaksen, K., Ishikawa, M., Johansson, M., Johannsson, H.,](#)
851 [Joo, A., Kaverin, D., Kholodov, A., Konstantinov, P., Kröger, T., Lambiel, C., Lanckman, J. P.,](#)
852 [Luo, D., Malkova, G., Meiklejohn, I., Moskalenko, N., Oliva, M., Phillips, M., Ramos, M.,](#)
853 [Sannel, A. B. K., Sergeev, D., Seybold, C., Skryabin, P., Vasiliev, A., Wu, Q., Yoshikawa, K.,](#)
854 [Zheleznyak, M., and Lantuit, H.: Permafrost is warming at a global scale, *Nature*](#)
855 [Communications, 10: 264, <https://doi.org/10.1038/s41467-018-08240-4>, 2019.](#)
- 856 Bockheim, J. G.: Importance of cryoturbation in redistributing organic carbon in permafrost-affected
857 soils, *Soil Sci. Soc. Am. J.* 71(4), 1335–1342, <https://doi.org/10.2136/sssaj2006.0414N>, 2007.

- 858 Brown, J., Ferrians Jr., O. J., Heginbottom, J. A., and Melnikov, E. S.: Circum-Arctic map of
859 permafrost and ground-ice conditions, 1 : 10 000 000, Map CP-45, United States Geological
860 Survey, International Permafrost Association, Washington, D. C., 1997.
- 861 Burke, E. J., Hartley, I. P., and Jones, C. D.: Uncertainties in the global temperature change caused
862 by carbon release from permafrost thawing, *The Cryosphere*, 6, 1063–1076,
863 <https://doi.org/10.5194/tc-6-1063-2012>, 2012.
- 864 Čapek, P., Diáková, K., Dickopp, J. E., Bárta, J., Wild, B., Schnecker, J., and Hugelius, G.: The
865 effect of warming on the vulnerability of subducted organic carbon in arctic soils, *Soil Biol.*
866 *Biochem.*, 90, 19–29, <https://doi.org/10.1016/j.soilbio.2015.07.013>, 2015.
- 867 Ciais, P.: A geoscientist is astounded by Earth’s huge frozen carbon deposits, *Nature*, 462, 393,
868 <https://doi.org/10.1038/462393e>, 2009.
- 869 Clymo, R. S. and Hayward, P. M.: The Ecology of *Sphagnum*, in: Smith, A. J. E. (ed). *Bryophyte*
870 *Ecology*. 540, 229–289, https://doi.org/10.1007/978-94-009-5891-3_8, 1982.
- 871 Davidson, E. A. and Janssens, I. A.: Temperature sensitivity of soil carbon decomposition and
872 feedbacks to climate change, *Nature*, 440, 165–173, <https://doi.org/10.1038/nature04514>, 2006.
- 873 [Diáková, K., Čapek, P., Kohoutová, I., Mpamah, P., Barta, J., Biasi, C., Martikainen, P., and](#)
874 [Šantrůčková, H.: Heterogeneity of carbon loss and its temperature sensitivity in East-European](#)
875 [subarctic tundra soils, *FEMS Microbiol. Ecol.*, 92: fiw140,](#)
876 [<https://doi.org/10.1093/femsec/fiw140>, 2016](#)
- 877 Elberling, B., Michelsen, A., Schädel, C., Schuur, E. A., Christiansen, H. H., Berg, L., Tamstorf, M.
878 P., and Sigsgaard, C.: Long-term CO₂ production following permafrost thaw, *Nature Climate*
879 *Change*, 3(10), 890–894, <https://doi.org/10.1038/nclimate1955>, 2013.
- 880 Faucherre, S., Jørgensen, C. J., Blok, D., Weiss, N., Siewert, M. B., Bang-Andreasen, T., Hugelius,
881 G., Kuhry, P., and Elberling, B.: Short and long-term controls on active layer and permafrost
882 carbon turnover across the Arctic, *J. Geophys. Res.--Biogeosciences.*, 123(2), 372–390.,
883 <https://doi.org/10.1002/2017JG004069>, 2018.
- 884 Fierer, N. and Schimel, J. P.: A proposed mechanism for the pulse in carbon dioxide production
885 commonly observed following the rapid rewetting of a dry soil. *Soil Sci. Soc. Am. J.*, 67(3),
886 798–805, <https://doi.org/10.2136/sssaj2003.0798>, 2003.
- 887 Franzluebbers, A. J., Haney, R. L., Honeycutt, C. W., Schomberg, H. H., and Hons, F. M.: Flush of
888 carbon dioxide following rewetting of dried soil relates to active organic pools, *Soil Sci. Soc.*
889 *Am. J.*, 64(2), 613–623, <https://doi.org/10.2136/sssaj2000.642613x>, 2000.
- 890 Gentsch, N., Mikutta, R., Alves, R. J. E., Barta, J., Čapek, P., Gittel, A., Hugelius, G., Kuhry, P.,
891 Lashchinskiy, N., Palmtag, J., Richter, A., Šantrůčková, H., Schnecker, J., Shibistova, O., Urich,
892 T., Wild, B., and Guggenberger, G.: Storage and transformation of organic matter fractions in
893 cryoturbated permafrost soils across the Siberian Arctic, *Biogeosciences*, 12(14): 4525–4542,
894 <https://doi.org/10.5194/bg-12-4525-2015>, 2015a.
- 895 [Gentsch, N., Mikutta, R., Shibistova, O., Wild, B., Schnecker, J., Richter, A., and Guggenberger, G.:](#)
896 [Properties and bioavailability of particulate and mineral-associated organic matter in Arctic](#)
897 [permafrost soils, Lower Kolyma Region, Russia. *European J. Soil Sci.*, 66: 722–734,](#)
898 [<https://doi.org/10.1111/ejss.12269>, 2015b.](#)
- 899 [Gentsch, N., Wild, B., Mikutta, R., Čapek, P., Diáková, K., Schrumppf, M., Turner, S., Minnich, C.,](#)
900 [Schaarschmidt, F., Shibistova, O., Schnecker, J., Urich, T., Gittel, A., Šantrůčková, H., Bárta, J.,](#)
901 [Lashchinskiy, N., Fuß, R., Richter, A., and Guggenberger, G.: Temperature response of](#)
902 [permafrost soil carbon is attenuated by mineral protection. *Glob. Change Biol.*, 24: 3401–3415,](#)
903 [<https://doi.org/10.1111/gcb.14316>, 2018.](#)

- 904 Gittel, A., Bárta, J., Kohoutová, I., Mikutta, R., Owens, S., Gilbert, J., Schnecker, J., Wild, B.,
905 Hannisdal, B., Maerz, J., Lashchinskiy, N., Čapek, P., Šantrůčková, H., Gentsch, N., Shibistova,
906 O., Guggenberger, G., Richter, A., Torsvik, V. L., Schleper, C., and Urich, T.: Distinct microbial
907 communities associated with buried soils in the Siberian tundra, *ISME J.*, 8, 841–853, 2014.
- 908 Grosse, G., Harden, J., Turetsky, M. R., McGuire, A. D., Camill, P., Tarnocai, C., Frolking, S.,
909 Schuur, E. A. G., Jorgenson, T., Marchenko, S., Romanovsky, V., Wickland, K. P., French, N.,
910 Waldrop, M. P., Bourgeau-Chavez, L., and Striegl, R. G.: Vulnerability of high-latitude soil
911 organic carbon in North America to disturbance, *J. Geophys. Res.*, 116, G00K06,
912 <https://doi.org/10.1029/2010JG001507>, 2011.
- 913 Grosse, G., Robinson, J. E., Bryant, R., Taylor, M. D., Harper, W., DeMasi, A., Kyker-Snowman, E.,
914 Veremeeva, A., Schirrmeister, L., and Harden, J.: Distribution of late Pleistocene ice-rich
915 syngenetic permafrost of the Yedoma suite in east and central Siberia, Russia, U. S. Geological
916 Survey Open File Report, 1078, 37 pp., 2013.
- 917 Gruber, N., Friedlingstein, P., Field, C. B., Valentini, R., Heimann, M., Richey, J. E., Romero-
918 Lankao, P., Schulze, D., and Chen, C.-T. A.: The vulnerability of the carbon cycle in the 21st
919 century: An assessment of carbon-climate-human interactions, in: *The Global Carbon Cycle,*
920 *Integrating Humans, Climate and the Natural World*, edited by: Field, C. and Raupach, M.,
921 Island Press, Washington D. C., 45–76, 2004.
- 922 Hammer, Ø., Harper, D.A.T., and Ryan, P. D.: PAST: Paleontological Statistics Software Package
923 for Education and Data Analysis. *Palaeontologia Electronica*, 4(1), 9 pp., 178kb, [http://palaeo-](http://palaeo-electronica.org/2001_1/past/issue1_01.htm)
924 [electronica.org/2001_1/past/issue1_01.htm](http://palaeo-electronica.org/2001_1/past/issue1_01.htm), 2001.
- 925 Harden, J. W., Koven, C. D., Ping, C. L., Hugelius, G., McGuire, A. D., Camill, P., Jorgenson, T.,
926 Kuhry, P., Michaelson, G. J., O'Donnell, J. A., Schuur, E. A. G., Tarnocai, C., Johnson, K., and
927 Grosse, G.: Field information links permafrost carbon to physical vulnerabilities of thawing,
928 *Geophys. Res. Lett.*, 39, L15704 <https://doi.org/10.1029/2012gl051958>, 2012.
- 929 Horwath Burnham, J. and Sletten, R. S.: Spatial distribution of soil organic carbon in northwest
930 Greenland and underestimates of High Arctic carbon stores, *Global Biogeochem. Cy.*, 24,
931 GB3012, <https://doi.org/10.1029/2009GB003660>, 2010.
- 932 Hugelius, G. and Kuhry, P.: Landscape partitioning and environmental gradient analyses of soil
933 organic carbon in a permafrost environment, *Global Biogeochem. Cy.*, 23, GB3006,
934 <https://doi.org/10.1029/2008GB003419>, 2009.
- 935 Hugelius, G., Kuhry, P., Tarnocai, C., and Virtanen, T.: Soil organic carbon pools in a periglacial
936 landscape: a case study from the central Canadian Arctic, *Permafrost Periglac.*, 21, 16–29,
937 <https://doi.org/10.1002/ppp.677>, 2010.
- 938 Hugelius, G., Virtanen, T., Kaverin, D., Pastukhov, A., Rivkin, F., Marchenko, S., Romanovsky, V.,
939 and Kuhry, P.: High-resolution mapping of ecosystem carbon storage and potential effects of
940 permafrost thaw in periglacial terrain, European Russian Arctic, *J. Geophys. Res.*, 116, G03024,
941 <https://doi.org/10.1029/2010JG001606>, 2011.
- 942 Hugelius, G., Strauss, J., Zubrzycki, S., Harden, J. W., Schuur, E. A. G., Ping, C.-L., Schirrmeister,
943 L., Grosse, G., Michaelson, G. J., Koven, C. D., O'Donnell, J. A., Elberling, B., Mishra, U.,
944 Camill, P., Yu, Z., Palmtag, J., and Kuhry, P.: Estimated stocks of circumpolar permafrost
945 carbon with quantified uncertainty ranges and identified data gaps, *Biogeosciences*, 11, 6573–
946 6593, <https://doi.org/10.5194/bg-11-6573-2014>, 2014.
- 947 Hugelius, G., Kuhry, P., and Tarnocai, C.: Ideas and perspectives: Holocene thermokarst sediments
948 of the Yedoma permafrost region do not increase the northern peatland carbon pool.
949 *Biogeosciences*, 13, 2003–2010, <https://doi.org/10.5194/bg-13-2003-2016>, 2016.

950 IPCC: Summary for Policymakers, in: Climate Change 2013: The Physical Science Basis.
 951 Contribution of Working Group I to the Fifth Assessment Report of the Intergovernmental Panel
 952 on Climate Change, edited by: Stocker, T. F., Qin, D., Plattner, G.-K., Tignor, M., Allen, S. K.,
 953 Boschung, J., Nauels, A., Xia, Y., Bex, V., and Midgley, P. M., Cambridge University Press,
 954 Cambridge, United Kingdom and New York, NY, USA, 2013.

955 [IPCC: Summary for Policymakers, in: Global Warming of 1.5 °C. An IPCC Special Report on the](#)
 956 [impacts of global warming of 1.5°C above pre-industrial levels and related global greenhouse](#)
 957 [gas emission pathways, in the context of strengthening the global response to the threat of](#)
 958 [climate change, sustainable development, and efforts to eradicate poverty, edited by Masson-](#)
 959 [Delmotte, V., Zhai, P., Pörtner, H.-O., Roberts, D., Skea, J., Shukla, P. R., Pirani, A.,](#)
 960 [Moufouma-Okia, W., Péan, C., Pidcock, R., Connors, S., Matthews, J. B. R., Chen, Y., Zhou,](#)
 961 [X., Gomis, M. I., Lonnoy, E., Maycock, T., Tignor, M., and Waterfield, T., World](#)
 962 [Meteorological Organization, Geneva, Switzerland, 32 pp., 2018.](#)

963 [Jarvis, P., Rey, A., Petsikos, C., Wingate, L., Rayment, M., Pereira, J., Banza, J., David, J., Miglietta,](#)
 964 [F., Borghetti, M., Manca, G. and Valentini, R.: Drying and wetting of Mediterranean soils](#)
 965 [stimulates decomposition and carbon dioxide emission: the “Birch effect”, Tree Physiology, 27:](#)
 966 [929–940, 2007.](#)

967 [Kaiser, C., Meyer, H., Biasi, C., Rusalimova, O., Barsukov, P., and Richter, A.: Conservation of soil](#)
 968 [organic matter through cryoturbation in arctic soils in Siberia, J. Geophys. Res., 112, G02017,](#)
 969 <https://doi.org/10.1029/2006JG000258>, 2007.

970 [Knoblauch, C., Beer, C., Sosnin, A., Wagner, D. and Pfeiffer, E.-M.: Predicting long-term carbon](#)
 971 [mineralization and trace gas production from thawing permafrost of Northeast Siberia, Glob.](#)
 972 [Change Biol., 19, 1160–1172, https://doi.org/10.1111/gcb.12116, 2013.](#)

973 [Kuhry, P.: The role of fire in the development of *Sphagnum*-dominated peatlands in Western Boreal](#)
 974 [Canada, J. Ecol., 82\(4\): 899-910, http://www.jstor.org/stable/2261453, 1994.](#)

975 Kuhry, P. and Vitt, D. H.: Fossil carbon/nitrogen ratios as a measure of peat decomposition, Ecology,
 976 77, 271–275, <https://doi.org/10.2307/2265676>, 1996.

977 Kuhry, P., Dorrepaal, E., Hugelius, G., Schuur, E. A. G., and Tarnocai, C.: Potential remobilization
 978 of belowground permafrost carbon under future global warming, Permafrost Periglac., 21, 208–
 979 214, <https://doi.org/10.1002/ppp.684>, 2010.

980 NCSCDv2: Doi:10.5879/ECDS/00000002, 2014.

981 Olefeldt, D., Turetsky, M. R., Crill, P. M., and McGuire, A. D.: Environmental and physical controls
 982 on northern terrestrial CH₄ emissions across permafrost zones, Glob. Change Biol., 19, 589–
 983 603, <https://doi.org/10.1111/gcb.12071>, 2013.

984 Palmtag, J., Hugelius, G., Lashchinskiy, N., Tamstorf, M. P., Richter, A., Elberling, B., and Kuhry,
 985 P.: Storage, landscape distribution and burial history of soil organic matter in contrasting areas
 986 of continuous permafrost, Arct. Antarct. Alp. Res., 47, 71–88,
 987 <https://doi.org/10.1657/AAAR0014-027>, 2015.

988 Palmtag, J., Ramage, J., Hugelius, G., Gentsch, N., Lashchinskiy, N., Richter, A., and Kuhry, P.:
 989 Controls on the storage of organic carbon in permafrost soils in northern Siberia, Eur. J. Soil
 990 Sci., 67, 478–491, <https://doi.org/10.1111/ejss.12357>, 2016.

991 Palmtag, J. and Kuhry, P.: Grain size controls on cryoturbation and soil organic carbon density in
 992 permafrost-affected soils, Permafrost Periglac., 29, 112–120, <https://doi.org/10.1002/ppp.1975>,
 993 2018.

994 Ping, C.-L., Michaelson, G. J., Jorgenson, M. T., Kimble, J. M., Epstein, H., Romanovsky, V. E., and
 995 Walker, D. A.: High stocks of soil organic carbon in North American Arctic region, Nat.
 996 Geosci., 1, 615–619, <https://doi.org/10.1038/ngeo284>, 2008.

- 997 Šantrůčková, H., Kurbatova, J., Shibistova, O., Smejkalova, M., and Kastovska, E.: Short-Term
998 Kinetics of Soil Microbial Respiration – A General Parameter Across Scales ? In: *Tree Species*
999 *Effects on Soils: Implications for Global Change*, Proceedings of the NATO Advanced Research
1000 Workshop on Trees and Soil Interactions, Implications to Global Climate Change, August 2004,
1001 Krasnoyarsk, Russia, pp. 229-246, https://doi.org/10.1007/1-4020-3447-4_13, 2006.
- 1002 Schuur, E. A. G., Bockheim, J., Canadell, J. G., Euskirchen, E., Field, C. B., Goryachkin, S. V.,
1003 Hagemann, S., Kuhry, P., Lafleur, P. M., Lee, H., Mazhitova, G., Nelson, F. E., Rinke, A.,
1004 Romanovsky, V. E., Shiklomanov, N., Tarnocai, C., Venevsky, S., Vogel, J. G., and Zimov, S.
1005 A.: Vulnerability of Permafrost Carbon to Climate Change: Implications for the Global Carbon
1006 Cycle, *Bioscience*, 58(8), 701–714, <https://doi.org/10.1641/B580807>, 2008.
- 1007 Schuur, E. A. G., McGuire, A. D., Schädel, C., Grosse, G., Harden, J. W., Hayes D. J., Hugelius, G.,
1008 Koven, C. D., Kuhry, P., Lawrence, D. M., Natali, S. M., Olefeldt, D., Romanovsky, V. E.,
1009 Schaefer, K., Turetsky, M. R., Treat, C. C., and Vonk, J. E.: Climate change and the permafrost
1010 carbon feedback, *Nature*, 20, 171–179, <https://doi.org/10.1038/nature14338>, 2015.
- 1011 Schädel, C., Schuur, E. A. G., Bracho, R., Elberling, B., Knoblauch, C., Lee, H., Luo, Y., Shaver, G.
1012 R., and Turetsky, M. R.: Circumpolar assessment of permafrost C quality and its vulnerability
1013 over time using long-term incubation data, *Glob. Change Biol.*, 20, 641–652,
1014 <https://doi.org/10.1111/gcb.12417>, 2014.
- 1015 Shmelev, D., Veremeeva, A., Kraev, G., Kholodov, A., Spencer, R. G. M., and Walker, W. S.:
1016 Estimation and Sensitivity of Carbon Storage in Permafrost of North-Eastern Yakutia,
1017 *Permafrost. Periglac.*, 28, 379–390, <https://doi.org/10.1002/ppp.1933>, 2017.
- 1018 Siewert, M. B., Hugelius, G., Heim, B., and Faucherre, S.: Landscape controls and vertical
1019 variability of soil organic carbon storage in permafrost-affected soils of the Lena River Delta,
1020 *CATENA*, 147, 725–741, <https://doi.org/10.1016/j.catena.2016.07.048>, 2016.
- 1021 Siewert, M. B.: High-resolution digital mapping of soil organic carbon in permafrost terrain using
1022 machine learning: a case study in a sub-Arctic peatland environment, *Biogeosciences*, 15, 1663–
1023 1682, <https://doi.org/10.5194/bg-15-1663-2018>, 2018.
- 1024 Schneckner, J., Wild, B., Hofhansl, F., Eloy Alves, R. J., Bárta, J., Čapek, P., Fuchslueger, L.,
1025 Gentsch, N., Gittel, A., Guggenberger, G., Hofer, A., Kienzl, S., Knoltsch, A., Lashchinskiy, N.,
1026 Mikutta, R., Šantrůčková, H., Shibistova, O., Takriti, M., Urich, T., Weltin, G., and Richter, A.:
1027 Effects of soil organic matter properties and microbial community composition on enzyme
1028 activities in cryoturbated arctic soils, *PLoS ONE*, 9, e94076,
1029 <https://doi:10.1371/journal.pone.0094076>, 2014.
- 1030 Soil Survey Staff: *Keys to Soil Taxonomy*, Twelfth Edition, USDA Natural Resources Conservation
1031 Service, Washington, D.C., 2014.
- 1032 Strauss, J., Schirrmeister, L., Grosse, G., Wetterich, S., Ulrich, M., Herzsuh, U., and Hubberten,
1033 H.-W.: The deep permafrost carbon pool of the Yedoma region in Siberia and Alaska, *Geophys.*
1034 *Res. Lett.*, 40, 6165–6170, <https://doi.org/10.1002/2013GL058088>, 2013.
- 1035 Tarnocai, C., Canadell, J. G., Schuur, E. A. G., Kuhry, P., Mazhitova, G., and Zimov, S.: Soil
1036 organic carbon pools in the northern circumpolar permafrost region, *Global Biogeochem. Cy.*,
1037 23, GB2023, <https://doi.org/10.1029/2008GB003327>, 2009.
- 1038 Vardy, S. R., Warner, B. G., Turunen, J., and Aravena, R.: Carbon accumulation in permafrost
1039 peatlands in the Northwest Territories and Nunavut, Canada, *Holocene*, 10, 273–280,
1040 <https://doi.org/10.1191/095968300671749538>, 2000.
- 1041 Walter Anthony, K. M., Zimov, S. A., Grosse, G., Jones, M. C., Anthony, P. M., Iii, F. S. C., Finlay,
1042 J. C., Mack, M. C., Davydov, S., Frenzel, P., and Frolking, S.: A shift of thermokarst lakes from

1043 carbon sources to sinks during the Holocene epoch, *Nature*, 511, 452–456,
1044 <https://doi.org/10.1038/nature13560>, 2014.

1045 Weiss, N., Blok, D., Elberling, B., Hugelius, G., Jorgensen, C. J., Siewert, M. B., and Kuhry, P.:
1046 Thermokarst dynamics and soil organic matter characteristics controlling initial carbon release
1047 from permafrost soils in the Siberian Yedoma region, *Sediment. Geol.*, 340, 38–48,
1048 <https://doi.org/10.1016/j.sedgeo.2015.12.004>, 2016.

1049 Weiss, N., Faucherre, S., Lampiris, N., and Wojcik, R.: Elevation-based upscaling of organic carbon
1050 stocks in high Arctic permafrost terrain: A storage and distribution assessment for Spitsbergen,
1051 Svalbard, *Polar Research*, 36(1), <https://doi.org/10.1080/17518369.2017.1400363>, 2017.

1052 Weiss, N. and Kaal, J.: Characterization of labile organic matter in Pleistocene permafrost (NE
1053 Siberia), using Thermally assisted Hydrolysis and Methylation (THM-GC-MS), *Soil Biol.*
1054 *Biochem.*, 117, 203-213, <https://doi.org/10.1016/j.soilbio.2017.10.001>, 2018.

1055 Zechmeister-Boltenstern, S., Keiblinger, K. M., Mooshammer, M., Penuelas, J., Richter, A., Sardans,
1056 J., and Wanek, W.: The application of ecological stoichiometry to plant–microbial–soil organic
1057 matter transformations, *Ecol. Monographs*, 85, 133–155, <https://doi.org/10.1890/14-0777.1>,
1058 2015.

1059
1060

1061 Tables

1062

1063 Pages

1064

1065 Figures

1066

1067 Pages

1068

Table 1

	%C vs C/N	%C vs DBD	C/N vs DBD
Correlation	positive	negative	negative
PAGE21, All sites	0.53 (228)	0.67 (232)	0.57 (228)
CryoCarb 1-Kolyma	0.79 (418)	0.78 (413)	0.63 (413)
CryoCarb 2-Taymyr	0.64 (484)	0.69 (480)	0.47 (480)
CryoCarb 3-Seida	0.47 (71)	0.84 (79)	0.47 (71)

Table 2

	DBD vs C release/gdw	%C vs C release/gdw	C/N vs C release/gdw
Correlation	negative	positive	positive
PAGE21, All sites	0.52 (232)	0.45 (232)	0.34 (228)
CryoCarb 1-Kolyma	0.52 (404)	0.47 (406)	0.54 (406)
CryoCarb 2-Taymyr	0.41 (480)	0.33 (484)	0.48 (484)
CryoCarb 3-Seida	0.81 (78)	0.43 (78)	0.38 (70)

Table 3

a

	Pt	Min/CE	Min Mtn	Min Pty	Min Lowl	Alluv	Eol	PI Yed
PAGE21, All sites	0.24	0.29	0.99	1.51	1.44	1.44	1.68	
CryoCarb-Kolyma	4.83	6.72	17.8	15.3	19.7	22.0		11.5
CryoCarb-Taymyr	6.24			29.3	24.7	26.2		
CryoCarb-Seida	2,40			5.76	7.92			

b

	Pt	Min/CE	Min Mtn	Min Pty	Min Lowl	Alluv	Eol	PI Yed
PAGE21, All sites	0.17	0.20	0.69	1.05	1	1.00	1.17	
CryoCarb-Kolyma	0.25	0.34	0.90	0.78	1	1.12		0.58
CryoCarb-Taymyr	0.26			1.18	1	1.06		
CryoCarb-Seida	0.30			0.73	1			
Mean relative lability	0.24	0.27	0.80	0.94	1	1.06	1.17	0.58
S.D. relative lability	0.05	0.10	0.15	0.22		0.06		

Table 4

a

	AL_Min	AL_Ce	P_Min	P_Ce	AL_Pt	OL Ls	Min Ls	Min Ls	
AL_OL	< 0.001	0.0072	< 0.001	< 0.001	< 0.001	0.0493	< 0.001	< 0.001	AL_OL
AL_Min		0.5761	0.2217	0.5360	0.1887	< 0.001	0.6598	0.5682	AL_Min
AL_Ce			0.1464	0.1387	0.5186	0.0160	0.1956	0.7096	AL_Ce
P_Min				0.5570	0.0119	< 0.001	0.7353	0.0809	P_Min
P_Ce					0.0119	< 0.001	1.0000	0.1828	P_Ce
AL_Pt						0.0018	0.0518	0.1103	AL_Pt
AL_OL Ls							< 0.001	< 0.001	AL_OL Ls
AL_Min Ls								0.2500	AL_Min Ls

b

	AL_Min	AL_Ce	P_Min	P_Ce	AL_Pty	AL_Pt	P_Pt	Fr_Yed	Th_Yed	
AL_OL	0.3800	0.0027	0.0658	< 0.001	0.0255	< 0.001	< 0.001	< 0.001	< 0.001	AL_OL
AL_Min		< 0.001	0.011	< 0.001	0.0174	< 0.001	< 0.001	< 0.001	< 0.001	AL_Min
AL_Ce			0.1178	0.2318	0.8849	0.0083	< 0.001	0.3428	0.1653	AL_Ce
P_Min				< 0.001	0.1656	< 0.001	< 0.001	0.0017	< 0.001	P_Min
P_Ce					0.4539	0.0098	< 0.001	0.9258	0.2751	P_Ce
AL_Pty						0.0168	< 0.001	0.5059	0.2036	AL_Pty
AL_Pt							0.0440	< 0.001	0.0034	AL_Pt
P_Pt								< 0.001	< 0.001	P_Pt
Fr_Yed									0.1448	Fr_Yed

Figure 1

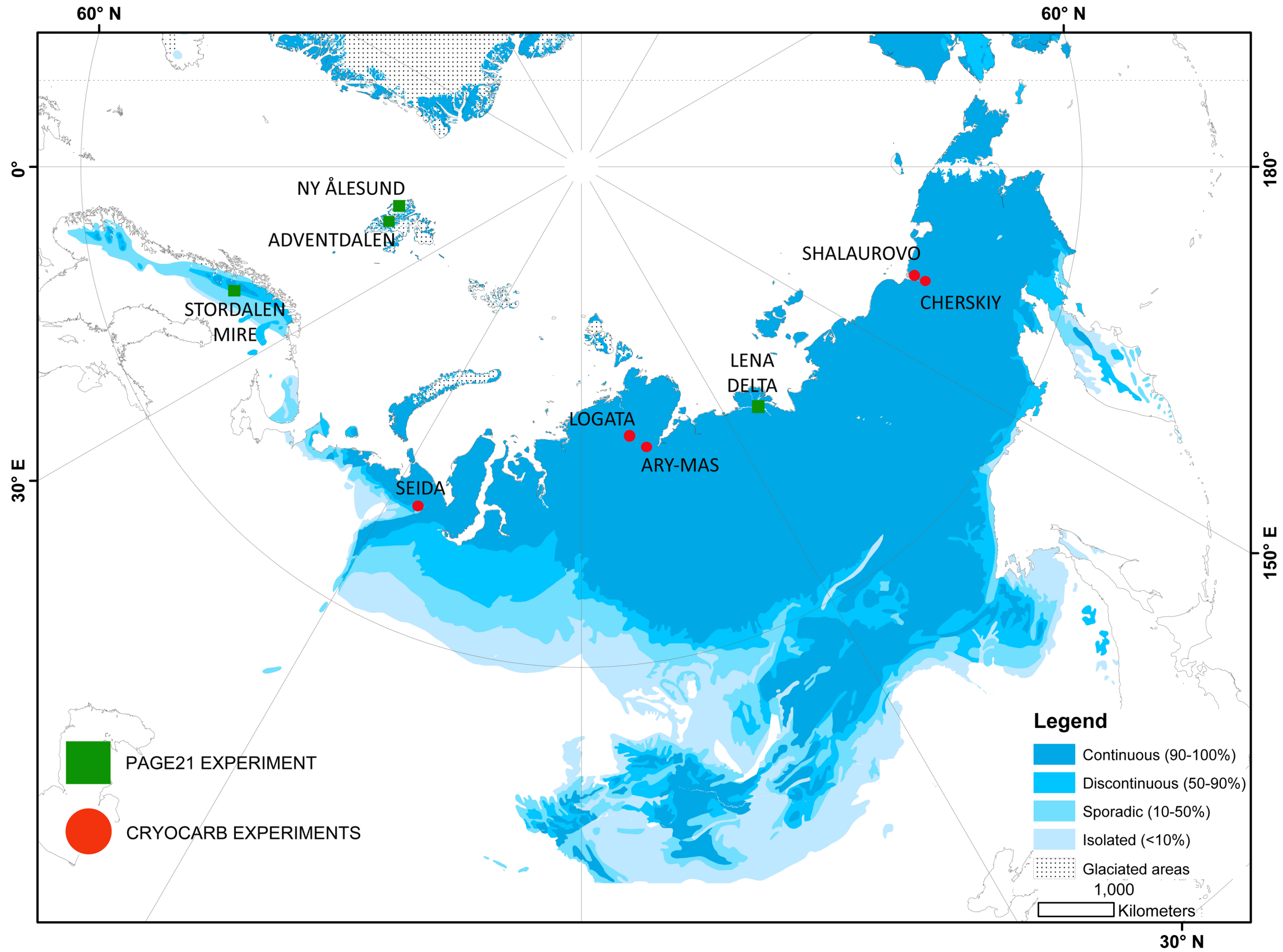
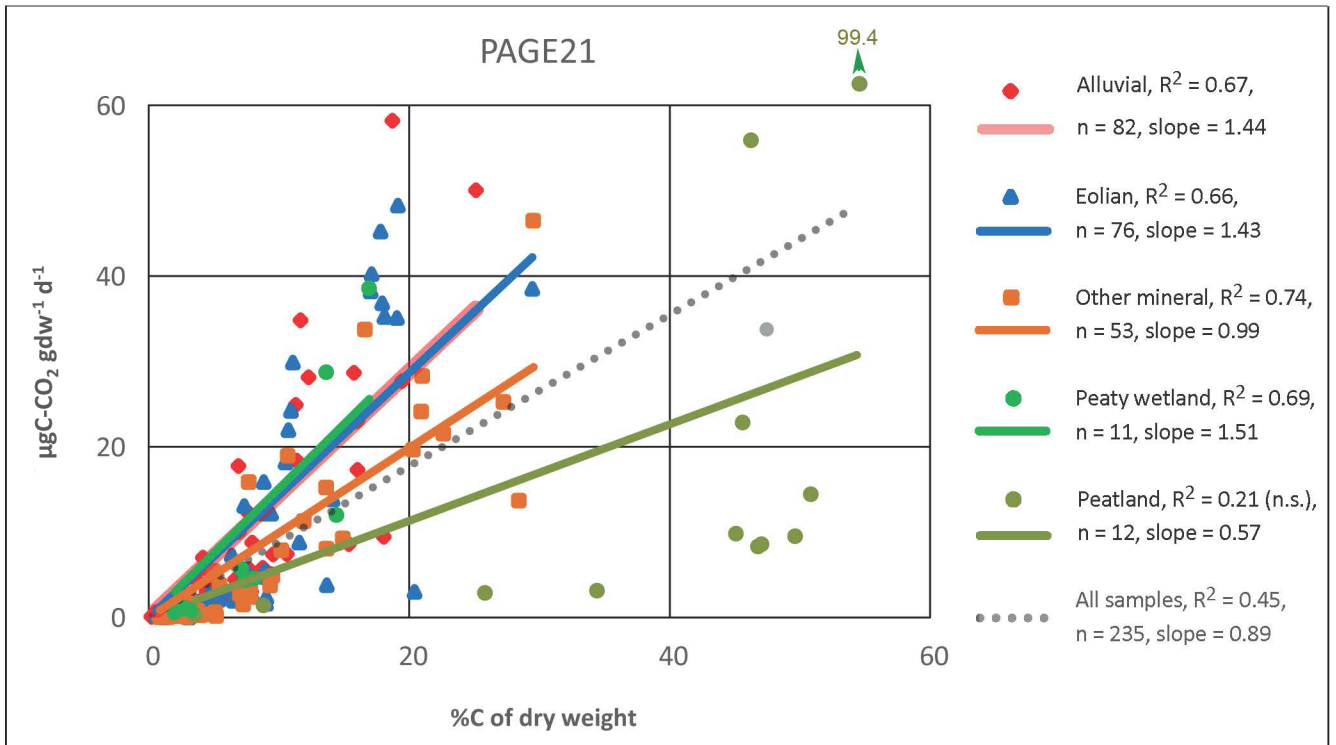


Figure 2

a



b

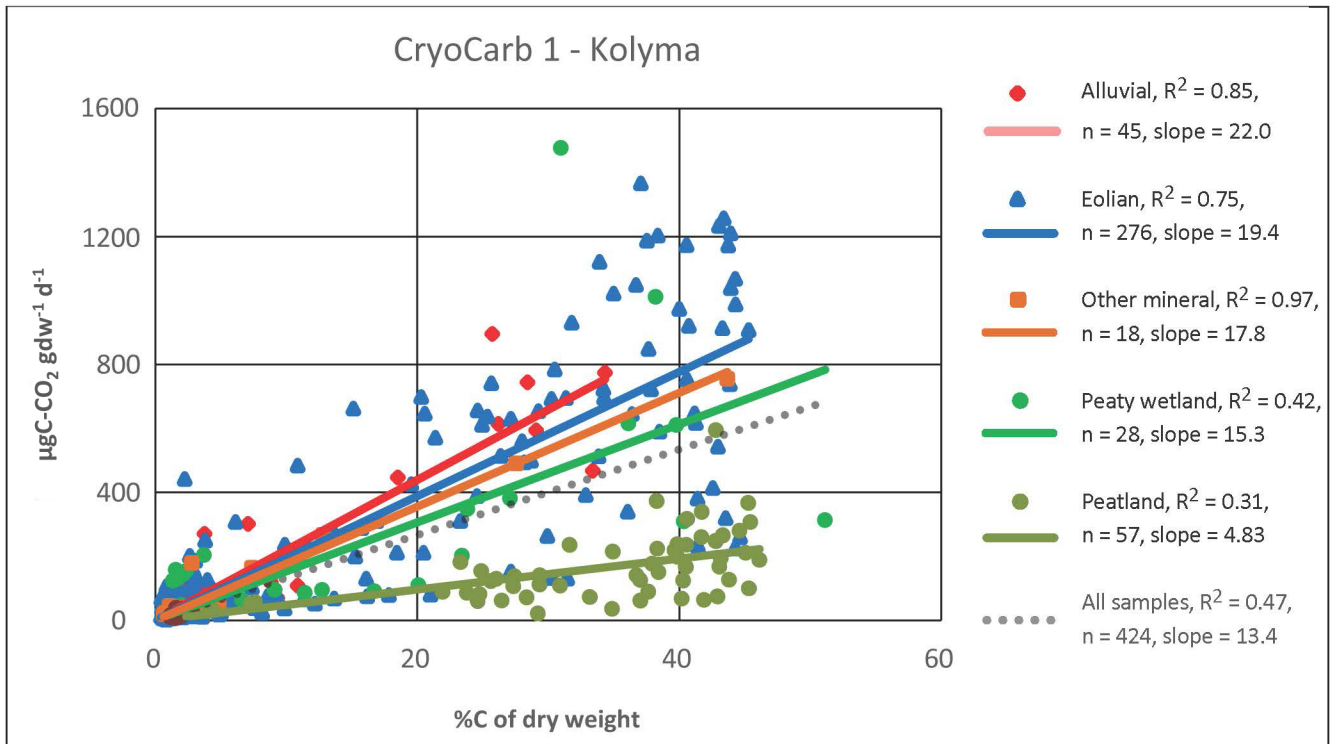
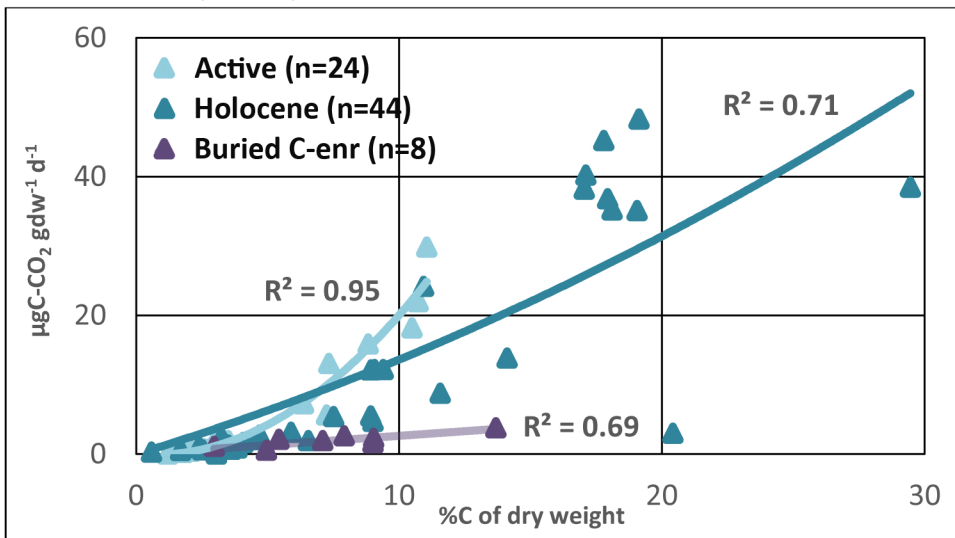
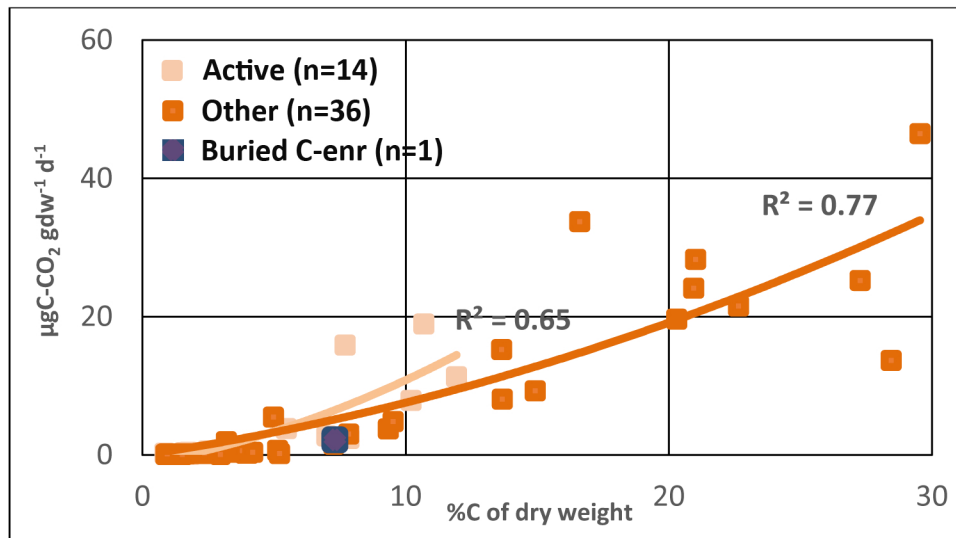


Figure 3

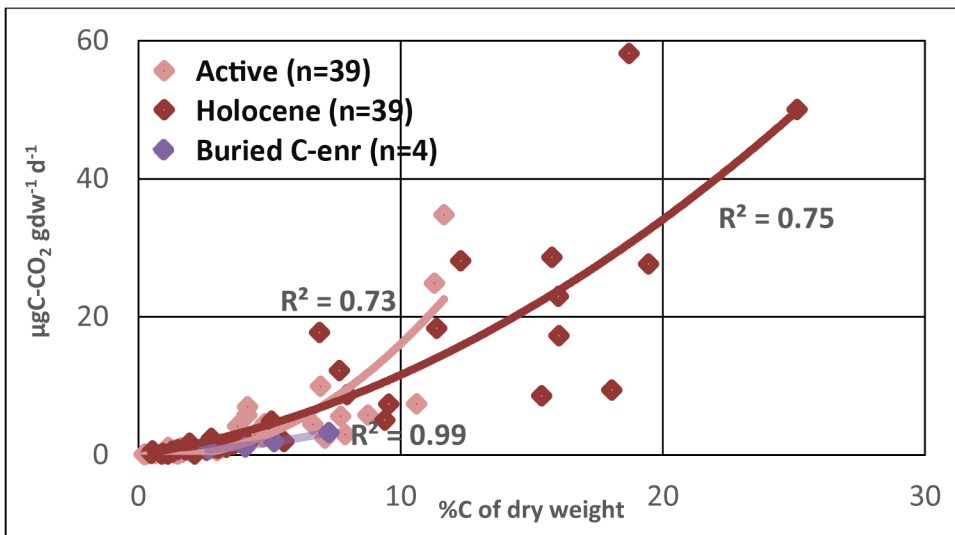
a. Eolian (n=76)



c. Mineral (n=51)



b. Alluvial (n=82)



d. Wetland (n=24)

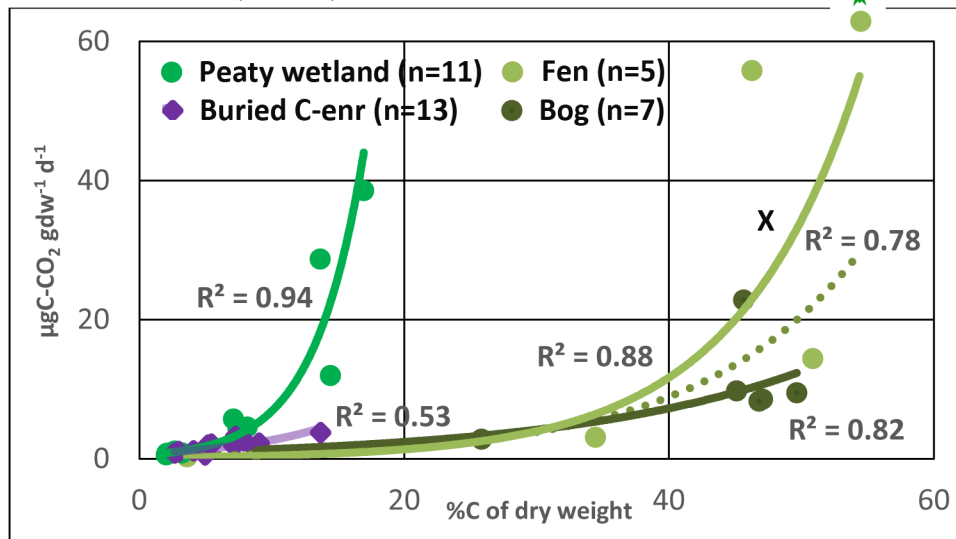
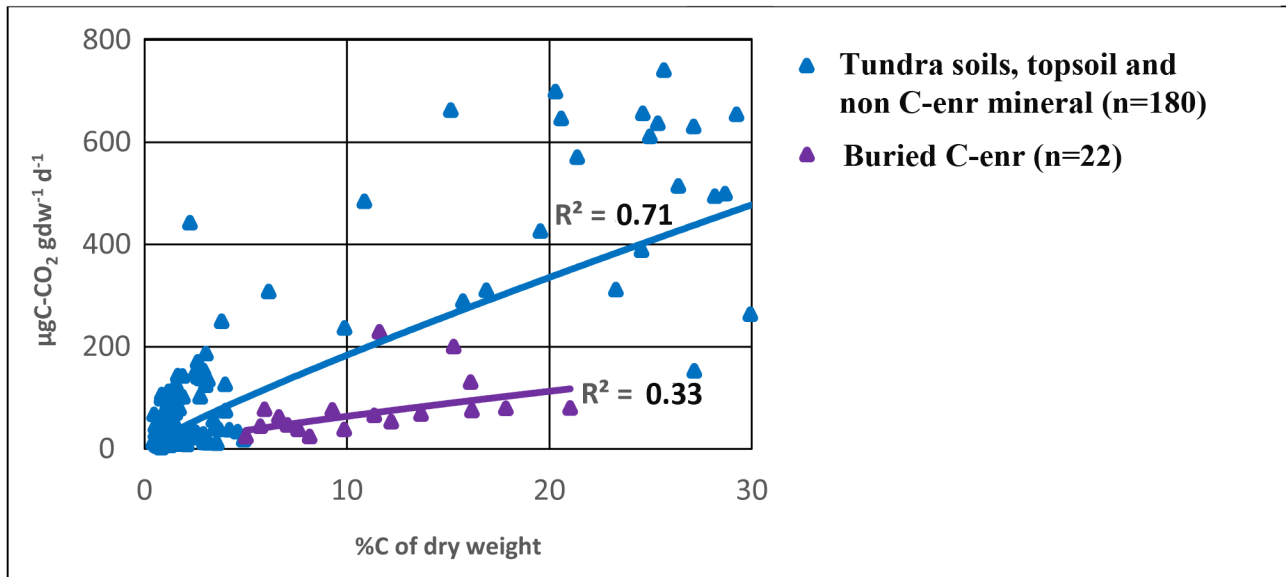


Figure 4

a



b

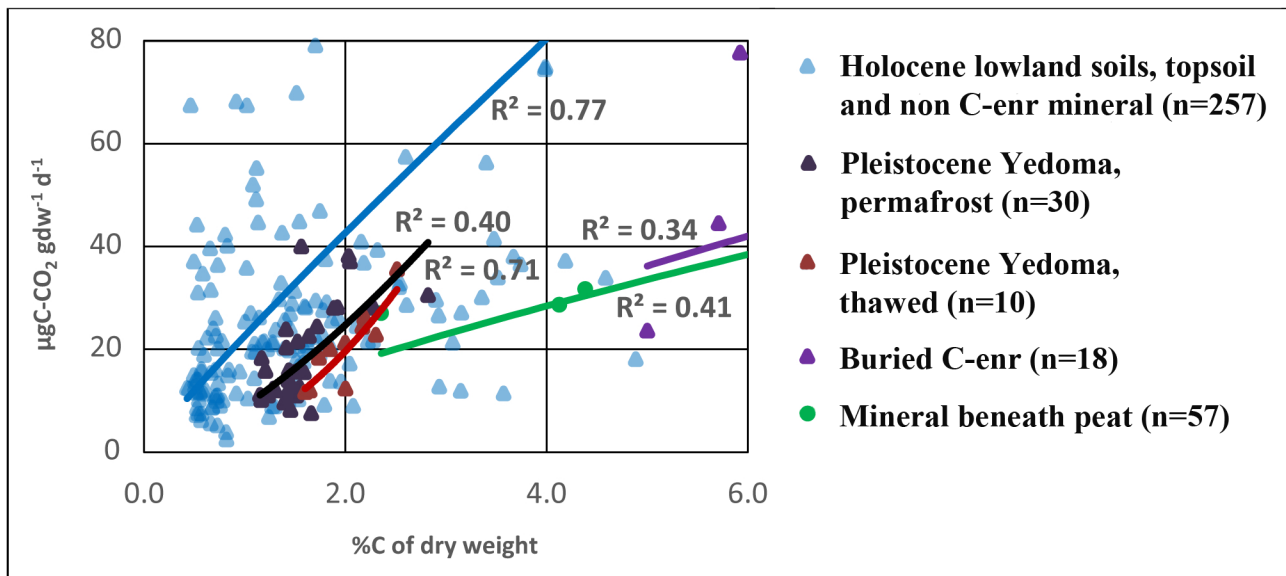
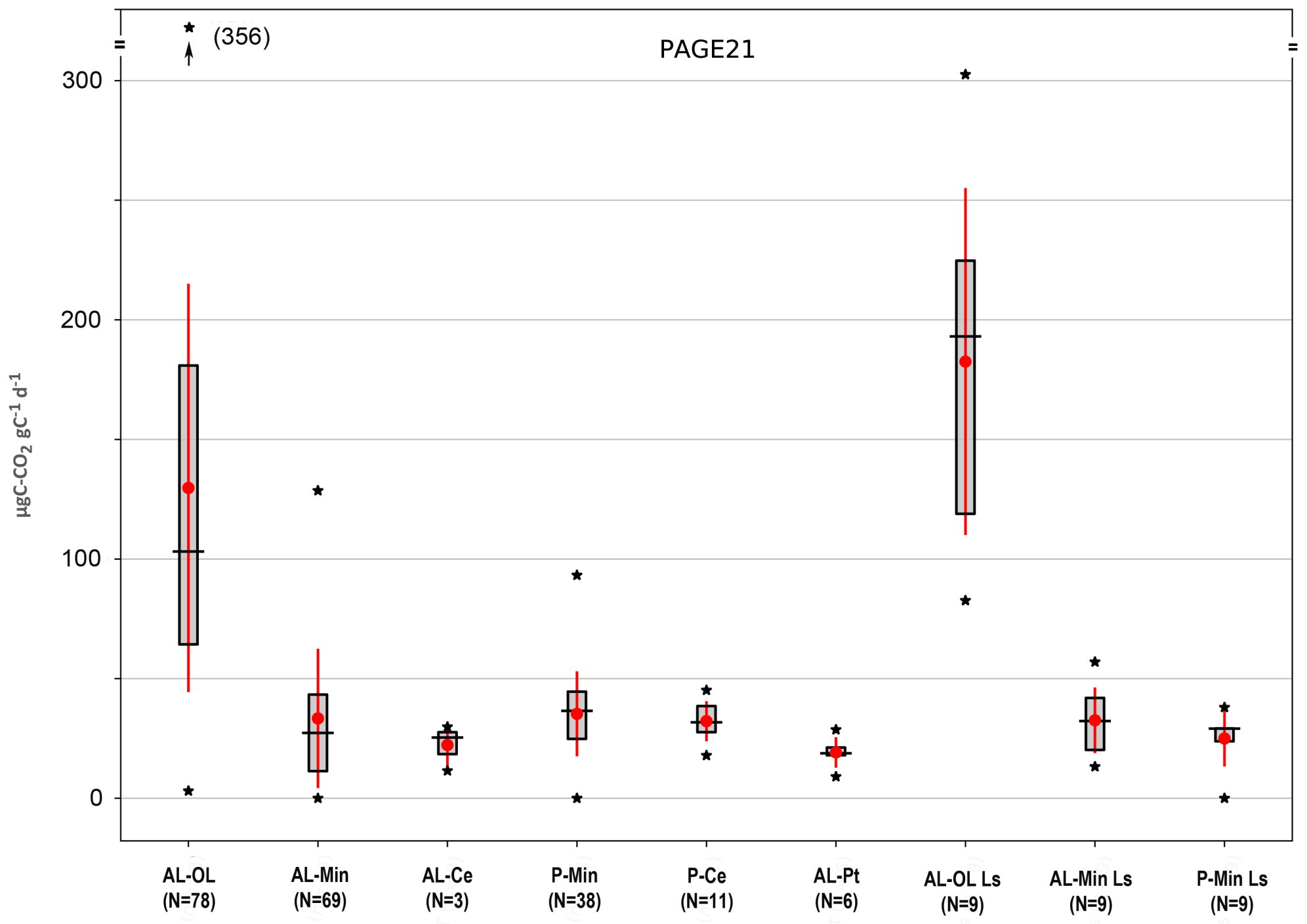


Figure 5

a



b

